

Palaeoclimate of the Late Jurassic of Portugal: comparison with the Western United States

TIMOTHY S. MYERS*, NEIL J. TABOR*, LOUIS L. JACOBS* and OCTÁVIO MATEUS†,‡

*Roy M. Huffington Department of Earth Sciences, Southern Methodist University, Dallas, TX 75275, USA (E-mail: smyers@mail.smu.edu)

†CICEGe, Faculdade de Ciências e Tecnologia, FCT, Universidade Nova de Lisboa, 2829-516 Caparica, Portugal

‡Museu da Lourinhã, Rua João Luis de Moura, 2530-157 Lourinhã, Portugal

Associate Editor – Adrian Immenhauser

ABSTRACT

Investigation of the palaeoclimatic conditions associated with Upper Jurassic strata in Portugal and comparison with published palaeoclimate reconstructions of the Upper Jurassic Morrison Formation in western North America provide important insights into the conditions that allowed two of the richest terrestrial faunas of this period to flourish. Geochemical analyses and observations of palaeosol morphology in the informally named Upper Jurassic Lourinhã formation of western Portugal indicate warm and wet palaeoclimatic conditions with strongly seasonal precipitation patterns. Palaeosol profiles are dominated by carbonate accumulations and abundant shrink-swell (vertic) features that are both indicative of seasonal variation in moisture availability. The $\delta^{18}\text{O}_{\text{SMOW}}$ and $\delta\text{D}_{\text{SMOW}}$ values of phyllosilicates sampled from palaeosol profiles range from +22.4‰ to +22.7‰ and –53.0‰ to –37.3‰, respectively. These isotope values correspond to temperatures of formation between 32°C and 39°C \pm 3°, with an average of 36°C, which suggest surface temperatures between 27°C and 34°C (average 31°C). On average, these surface temperature estimates are 1°C higher than the highest summer temperatures modelled for Late Jurassic Iberia using general circulation models. Elemental analysis of matrix material from palaeosol B-horizons provides proxy (chemical index of alteration minus potassium) estimates of mean annual precipitation ranging from 766 to 1394 mm/year, with an average of approximately 1100 mm/year. Palaeoclimatic conditions during deposition of the Lourinhã formation are broadly similar to those inferred for the Morrison Formation, except somewhat wetter. Seasonal variation in moisture availability does not seem to have negatively impacted the ability of these environments to support rich and relatively abundant faunas. The similar climate between these two Late Jurassic terrestrial ecosystems is probably one of the factors which explains the similarity of their vertebrate faunas.

Keywords Lourinhã formation, Lusitanian Basin, Morrison Formation, palaeoclimatology, palaeosols, stable isotopes.

INTRODUCTION

The Upper Jurassic terrestrial deposits of the Western United States have long been recognized as a rich source of vertebrate fossil remains,

including a diversity of dinosaurs (Foster, 2003). As a result of their palaeontological significance, the deposits of the Morrison Formation have benefited from extensive research into the palaeoclimate and palaeoenvironments that supported

such a large faunal community (Demko & Parrish, 1998; Dunagan, 2000; Demko *et al.*, 2004; Dunagan & Turner, 2004; Parrish *et al.*, 2004). Upper Jurassic strata in western Portugal preserve a terrestrial fauna similar in composition and richness to that of the Morrison Formation (Mateus, 2006; Mateus *et al.*, 2006) and have also attracted palaeontological interest for many years (Lapparent & Zbyszewski, 1957; Antunes & Mateus, 2003). Although the Portuguese fauna has been studied thoroughly, the local palaeoclimate under which this community flourished has yet to be detailed. The only significant palaeoclimate interpretations of the Upper Jurassic Portuguese terrestrial sequence are presented by Hill (1989) and Martinius & Gowland (2011), who inferred seasonal, semi-arid conditions from a combination of palaeoclimate modelling and sedimentological evidence. Given the superficial similarities between the Late Jurassic faunas of the Western United States and Portugal, these two areas are expected to have had similar palaeoclimates.

Many previous studies have explored global palaeoclimate in the Late Jurassic or described the rich faunas that flourished in various regions around the world at that time, but too little attention has been paid to understanding local to regional scale climate and how it may have permitted the establishment of these unique ecosystems. This study examines the Late Jurassic palaeoclimate of Portugal through the morphology and distribution of palaeosols in coastal outcrops of the informally named Lourinhã formation. Geochemical analyses are used to generate estimates of mean annual precipitation and surface temperature. These detailed palaeoclimate data from the Lourinhã formation are compared with previously published information from the Morrison Formation to determine whether these two deposits, that preserve such similar terrestrial faunas, also reflect similar palaeoclimates.

GEOLOGICAL BACKGROUND

Tectonic and palaeogeographic setting

During the Late Jurassic, northward propagation of sea floor spreading between the North American and Eurasian plates opened a series of marginal basins in the present-day North Atlantic (Uchupi, 1988; Golonka & Ford, 2000; Golonka, 2007). The region currently occupied by Western Europe consisted of a number of small islands

separated by shallow continental shelves that may have been emergent during lowstands (Upchurch *et al.*, 2002). Iberia was an isolated landmass, located at approximately 30°N palaeolatitude (Smith *et al.*, 1994; Golonka *et al.*, 1996). In North America, terrestrial strata of the Morrison Formation were deposited in the western half of the continent between 30°N and 35°N palaeolatitude (Smith *et al.*, 1994).

The study area is located in the Lusitanian Basin on the western coast of Portugal (Fig. 1). The basin, an extensional feature created by NNE to SSW trending normal faults active during opening of the North Atlantic (Wilson, 1975), served as a catchment for terrestrial sediments shed from Iberian highlands in the Late Jurassic (Hill, 1989). Approximately 250 km long by 100 km wide with an onshore area of 23 000 km², the Lusitanian Basin is bounded on its eastern margin by uplifted Late Palaeozoic basement rocks (Pena dos Reis *et al.*, 1996). To the west, much of the horst structure that once formed the western basin margin now lies submerged offshore, its position denoted by Berlenga and the Farilhões Islands (Wilson, 1988). The outcrops examined here are located in the Consolação sub-basin of the central Lusitanian Basin, bordered by the Nazaré Fault to the north and the Tagus Fault to the south.

Stratigraphy

The central Lusitanian Basin contains primarily Mesozoic deposits, with Upper Triassic to Upper Cretaceous rocks overlain by a veneer of Cenozoic deposits (Azerêdo *et al.*, 1998). Middle Jurassic marine units, including both clastics and shallow water carbonates (Wilson, 1988), are separated from Upper Jurassic deposits by a basin-wide disconformity that spans the Late Callovian to Early Oxfordian (Azerêdo *et al.*, 1998, 2002). Marine influence persists in lower Upper Jurassic deposits, but begins to wane in Upper Oxfordian strata (Jacquin *et al.*, 1998; Leinfelder & Wilson, 1998). Significant amounts of terrestrial sediments, contained within the informally named Lourinhã formation, first appear in the upper Kimmeridgian part of the succession and increase in areal extent and volume throughout the remainder of the Upper Jurassic sequence.

Formation of numerous sub-basins through a combination of faulting and halokinesis has created notable intrabasin stratigraphic heterogeneity, with adjacent sub-basins often preserving different stratigraphic successions (Ravnås *et al.*,

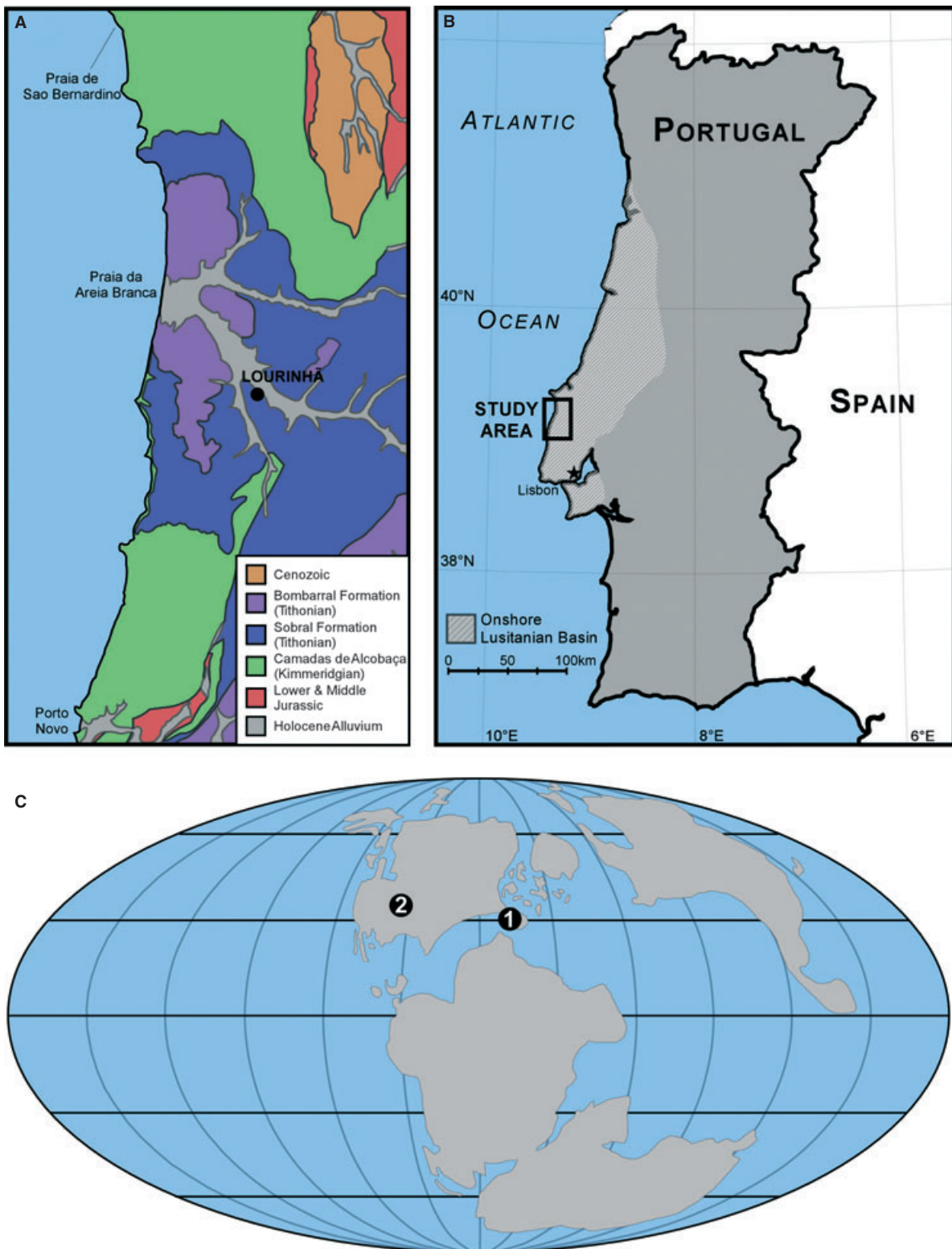


Fig. 1. Map of the study area showing local geology and palaeogeographic position. (A) Map of surficial geology on the Areia Branca syncline, centred at 39°267'N, 9°336'W. Map modified from Manuppella (1996). The Lourinhã formation as discussed here and originally proposed by Hill (1989) includes the Camadas de Alcobaça, the Sobral Formation and the Bombarral Formation (mapped in green, blue and purple). (B) Position of study area within the onshore portion of the Lusitanian Basin. (C) Palaeogeographic position of the Lourinhã formation (1) relative to the Morrison Formation (2). Modified from Smith *et al.* (1994).

1997; Alves *et al.*, 2003). This heterogeneity renders development of a single basinwide stratigraphy impossible. Hill (1988, 1989) first used the informal designation ‘Lourinhã formation’ to refer to the package of distal alluvial fan deposits exposed along the coastal cliffs of western Portugal between Sintra and Peniche, previously known as the Grés Superiores (Wilson, 1979; Leinfelder, 1986). The Lourinhã formation has been divided into five members, which are, in ascending stratigraphic order, the Praia da Amoreira, Porto Novo, Praia Azul, and stratigraphically equivalent Assenta and Santa Rita members (Hill, 1988, 1989). In the Consolação sub-basin, between the towns of São Bernardino and Porto Novo, only the Praia da Amoreira, Porto Novo and Praia Azul members are exposed (Hill, 1988, fig. 1·8). In this same area, the Serviços Geológicos de Portugal (Portuguese Geological Survey) recognizes three different formations: the Camadas de Alcobaça, the Sobral Formation and the Bombarral Formation (Manuppella, 1998). These three units are synonymous with the Lourinhã formation envisaged by Hill (1989).

Although the Lourinhã stratigraphy is not yet formalized, subsequent studies in the central Lusitanian Basin (Wilson *et al.*, 1989; Ravnås *et al.*, 1997; Leinfelder & Wilson, 1998; Alves *et al.*, 2003) have adopted the term Lourinhã formation as proposed by Hill (1989). For the purposes of this study, stratigraphic nomenclature will follow Hill (1989) and subsequent authors and refer to the Upper Jurassic terrigenous clastics exposed along the western coast of the Estremadura region as the Lourinhã formation.

Depositional setting and age

The Lourinhã formation comprises distal deposits of a low relief alluvial fan sourced from the now-submerged western margin of the Lusitanian Basin (Hill, 1989). Fluvial channel sandstones, finer-grained overbank deposits and floodplain mudstones are the primary components of the Lourinhã formation, and deltaic deposits are present near the base of the succession (Hill, 1989; Leinfelder & Wilson, 1998). The channel facies within the Lourinhã formation consists of thick, fine to coarse-grained, lenticular sandstones that show little evidence of lateral continuity. In some cases, channel bodies preserve lateral accretion sets, but more commonly display trough cross-stratification or planar bedding (Fig. 2). Channel deposits often contain carbonized plant material ranging in size

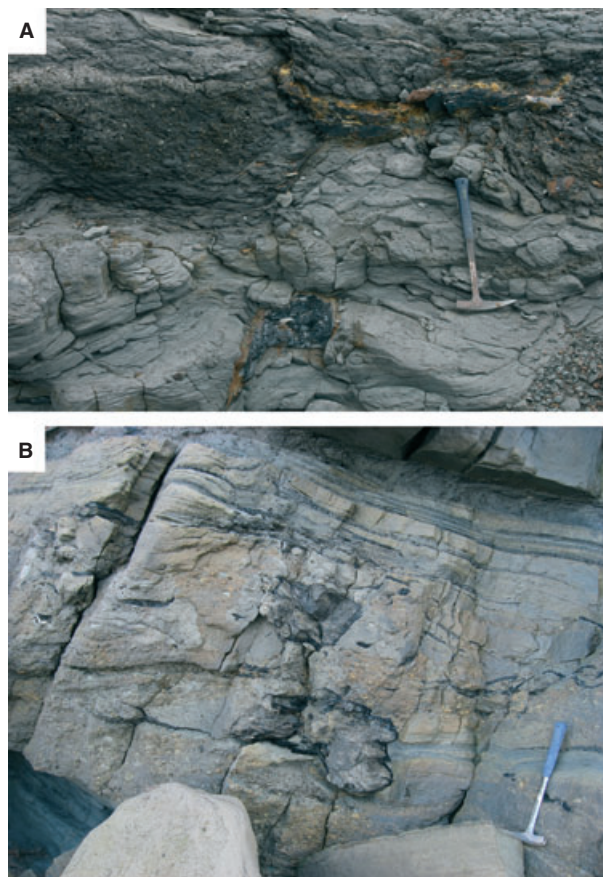


Fig. 2. Different types of organic preservation observed in the Lourinhã formation. (A) Compressed remains of large logs. (B) Mixture of wood fragments and seams of fine bits of plant material. Rock hammer (40·5 cm long) for scale.

from large logs several metres in length to small fragments of wood and lenses of fine particulate matter (Fig. 2). Pedogenically modified overbank mudstones are abundant in the Lourinhã formation and commonly display carbonate accumulations and shrink-swell (vertic) features. Despite the largely terrestrial nature of the Lourinhã formation (Wilson, 1979; Hill, 1989), sporadic marine influence is evident throughout the formation due to its close proximity to a shallow marine embayment (Martinius & Gowland, 2011). Thin shell lags deposited in a calcareous sandstone matrix appear at several levels within the formation (Fig. 3). These lag units, dominated by the bivalves *Isognomon lusitanicum*, *Eomiodon* and *Jurassicorbula*, are unquestionably marine (Fürsich, 1981). To the south, Lourinhã deposits interfinger with shallow marine carbonates of the Freixial and Arranhó members of the Farta Pão Formation (Leinfelder, 1993; Leinfelder & Wilson, 1998).

The Lourinhã formation in the Consolação sub-basin is estimated to be latest Kimmeridgian to



Fig. 3. Shell beds in the Lourinhã formation. (A) *Isognomon*-dominated bed from the northern section, (B) Detail of shell bed from the southern section. Rock hammer (40.5 cm long) for scale.

Tithonian in age (Leinfelder, 1993), although some studies suggest that parts of the formation may have been deposited as early as the Late Oxfordian or as late as the Early Berriasian (Alves *et al.*, 2002). Proposed ages for the Lourinhã beds are based on a biostratigraphic framework developed using ammonites (Marques *et al.*, 1996), ostracodes (Helmdach, 1973; Schudack *et al.*, 1998), charophytes (Pereira *et al.*, 2003) and palynomorphs (Mohr & Schmidt, 1988; Mohr, 1989). More recent biostratigraphic analysis of the Lourinhã formation, drawing on new micropalaeontological and palynological data, suggests a late Kimmeridgian age for much of the formation (Martinius & Gowland, 2011).

Correlation with the Morrison Formation

Deposition of the Lourinhã formation is roughly contemporaneous with that of the Morrison Formation of the Western United States (Fig. 4). The Morrison Formation consists primarily of fluvio-lacustrine deposits that crop out over an area

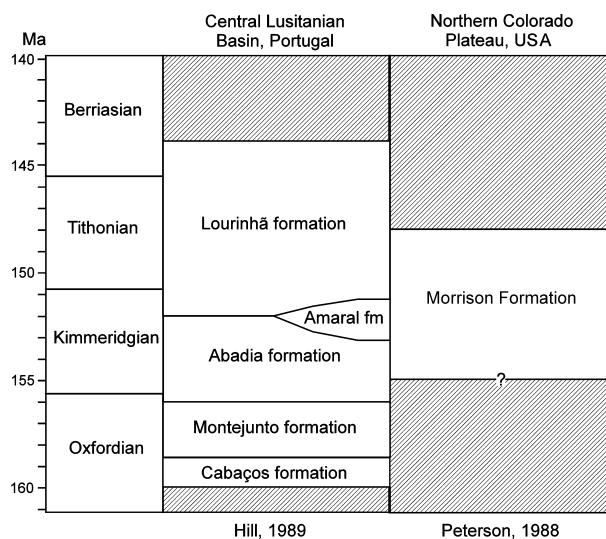


Fig. 4. Correlation chart for Upper Jurassic terrestrial successions of North America and Western Europe. The age of the Lourinhã formation is based on biostratigraphy (Hill, 1989). The age of the Morrison Formation is determined from radiometric dating (Kowallis *et al.*, 1998). Stratigraphy based on references listed at the bottom of chart (Peterson, 1988; Hill, 1989).

ranging from New Mexico north to Montana and from Utah east to Oklahoma (Foster, 2003; Turner & Peterson, 2004). Based on radiometric dating, the estimated age of the Morrison Formation is 155 to 148 Ma (Kowallis *et al.*, 1991, 1998), corresponding to an interval spanning most of the Kimmeridgian and the Early Tithonian (Gradstein *et al.*, 2005). Other dating methods, including charophyte and ostracode biostratigraphy (Schudack *et al.*, 1998) and magnetostratigraphy (Steiner, 1998) corroborate this age, and indicate that parts of the Morrison Formation may be Upper Oxfordian. Currie (1998) suggested that the top of the Morrison Formation may extend into the Lower Cretaceous based on a single K/Ar date of 135.2 ± 5.5 Ma, but this date conflicts with another K/Ar date from the same horizon that indicates a Late Jurassic age of 152.9 ± 1.2 Ma (Kowallis *et al.*, 1991). Based on the age information summarized here, late Kimmeridgian and Early Tithonian deposition of the Lourinhã formation was coeval with deposition of younger portions of the Morrison Formation.

METHODS

Field sampling and laboratory analysis

Two correlative, composite stratigraphic sections were measured (Fig. 5) along a broad syncline

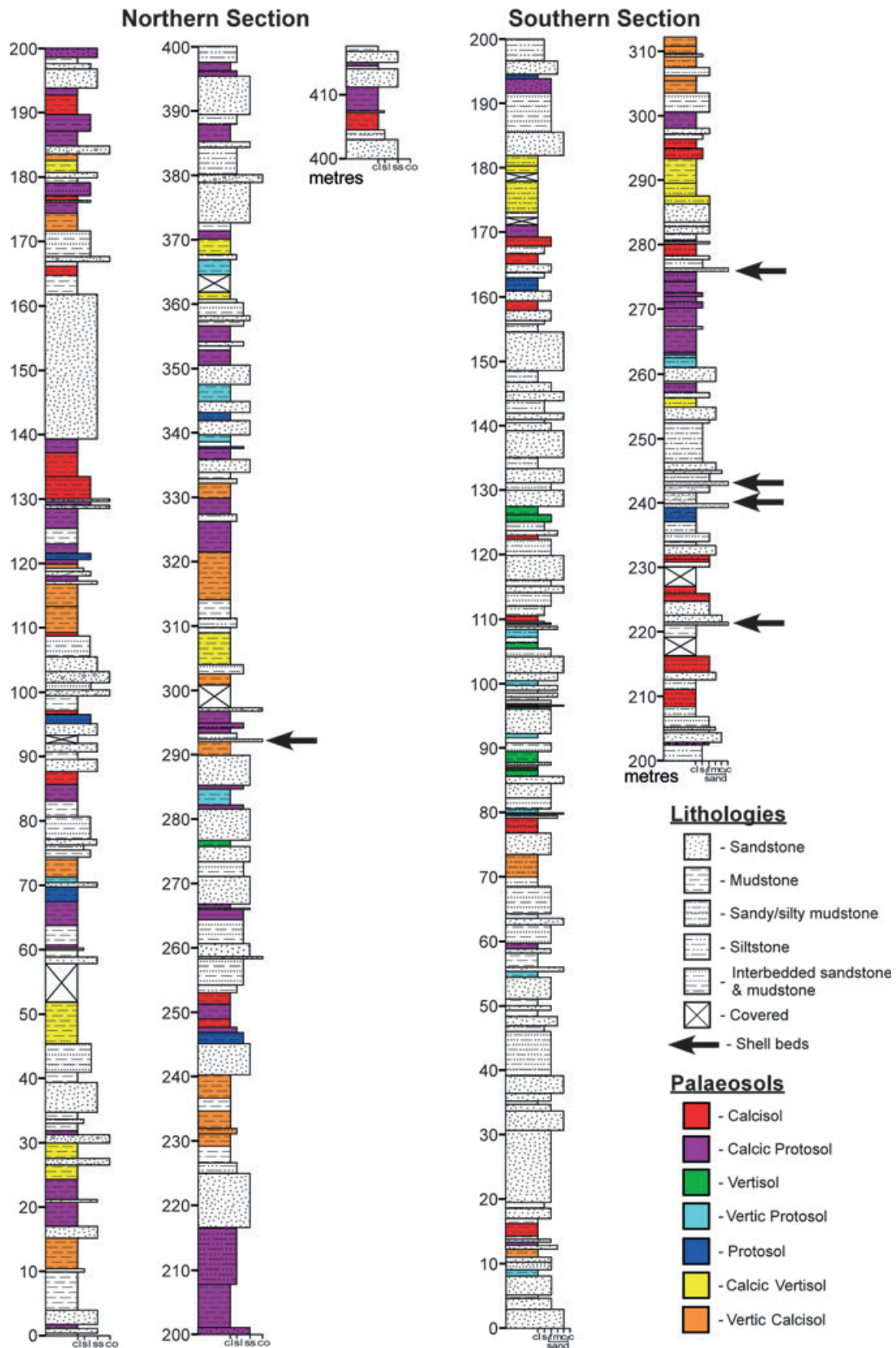


Fig. 5. Stratigraphic sections of the Lourinhã formation from the northern and southern limbs of the Areia Branca syncline showing the distribution of palaeosol types. Arrows indicate the positions of marine shell beds dominated by the bivalve *Isognomon*.

centred at the town of Areia Branca (39°26'7"N, 9°33'6"W). The section measured on the north limb is 415 m thick, and the section on the south limb measures 314 m. The northern section begins just north of Praia de São Bernardino at the base of the first mudstone unit above the last evidence of major marine influence, roughly corresponding with the northern coastal boundary of the Lourinhã formation as illustrated by Hill (1988, fig. 1·8; 1989, fig. 1). The section extends south for 5 km along the coast, ending at the northern edge of Praia de Areia Branca. The southern section begins approximately 10 km north-east of Porto Novo, just south of Praia de Valmitão, and runs 7 km north, ending at the southern edge of Praia de Areia Branca. One hundred palaeosols were described in the northern limb of the syncline, and 64 palaeosols were described in the southern section. Palaeosol descriptions included observations of colour, grain size, mottling, root abundance, ped structure, abundance and morphology of carbonate accumulations, and slickenside development. Palaeosols were classified using the taxonomic framework proposed by Mack *et al.* (1993). Bulk matrix samples and carbonate samples were collected from selected palaeosol B-horizons for subsequent analysis.

Selected matrix samples were prepared for X-ray diffraction (XRD) analysis by disaggregation in deionized water or dilute sodium carbonate solution, followed by centrifugation to isolate the clay fraction (<2 µm). Oriented aggregates were prepared on filter membranes and transferred to glass slides. Each clay sample was treated to produce potassium-saturated, magnesium-saturated, and magnesium-saturated as well as glycerol solvated mounts. After initial XRD analysis, potassium-saturated samples were heated in a furnace at 500°C for a minimum of two hours, and then reanalyzed. Analysis of the total clay fraction was followed by isolation and analysis of the fine clay fraction (<0·2 µm), which contains predominantly pedogenic, rather than detrital, clays (Stern *et al.*, 1997; Tabor *et al.*, 2002; Vitali *et al.*, 2002). All samples were analyzed at Southern Methodist University (SMU) using a Rigaku Ultima III X-ray diffractometer (Rigaku Corporation, Toyko, Japan) with a step size of 0·05° over a spectrum of 2 to 30° 2θ. Relative abundance of clay mineral constituents was estimated using the area of the 001 peak in the diffraction pattern of glycerol-solvated samples with background removed.

A subset of matrix samples was sent for X-ray fluorescence (XRF) analysis at the Center for

Applied Isotope Studies at the University of Georgia. These samples were analyzed for major elemental composition using the lithium-borate fusion method and a Philips (PANalytical) PW2420 wavelength-dispersive XRF spectrometer (Philips, Amsterdam, The Netherlands). Results were reported as oxide weight percentages, which were then normalized to their molecular weights. These data are used to calculate estimates of mean annual precipitation (MAP) using the chemical index of alteration minus potassium (CIA-K) as a proxy (Sheldon *et al.*, 2002).

Palaeotemperature estimates are derived from δ¹⁸O and δD analysis of pedogenic clay minerals based on the methods described by Clayton & Mayeda (1963) and Tabor & Montañez (2005). Four fine clay samples (<0·2 µm) from palaeosol B-horizons were selected for analysis. Each sample was treated with a citrate–bicarbonate–dithionite solution to remove iron oxides, rinsed with deionized water, dried in an oven at 40°C, and separated into two aliquots for δD and δ¹⁸O analyses. The fractions used for δD analysis were dehydrated under vacuum at ca 250°C to remove any adsorbed or interlayer water. Samples were then heated at ca 850°C to promote dehydroxylation of the clay minerals. The dehydroxylation process yielded water vapour, which was captured and purified cryogenically, then passed over uranium heated to ca 760°C to convert water vapour to hydrogen gas. The isotopic composition of the hydrogen gas was analyzed at SMU with a Finnigan MAT 252 isotope ratio mass spectrometer (Thermo-Fisher Scientific Corporation, Waltham, MA, USA). Sample fractions selected for δ¹⁸O analysis were also dehydrated to remove adsorbed or interlayer water. Samples were then reacted with BrF₅ at 560°C to produce oxygen gas, and the resultant O₂ was reacted with graphite to produce CO₂. The carbon dioxide was then cryogenically isolated and analyzed with a Finnigan MAT 252 isotope ratio mass spectrometer at SMU. Both δD and δ¹⁸O values are reported in per mil (‰) units relative to Standard Mean Ocean Water (SMOW).

RESULTS

Palaeosol classification

Approximately 45% of the stratigraphic thickness of the northern section and 28% of the southern section is composed of pedogenically altered

material. Based on the morphology, lithology, mineralogy and organization of the 164 profiles documented in the two stratigraphic sections, Lourinhã palaeosols are grouped into seven distinct types (Figs 5 and 6). Each palaeosol profile was evaluated to determine its most prominent pedogenic features and classified using the nine palaeosol orders and various subordinate modifiers developed by Mack *et al.* (1993). Variations of three palaeosol orders are observed: Protosols, Calcisols and Vertisols. Calcic Protosols are the most common palaeosol type in the northern

section, whereas Vertisols are the least common. Calcisols are most abundant in the southern section, while Protosols are the least abundant. The description, abundance and stratigraphic distribution of each palaeosol type are presented below.

Calcisols

Fourteen percent of the palaeosols in the northern section and 33% of the palaeosols in the southern section are Calcisols. Lourinhã Calcisol profiles

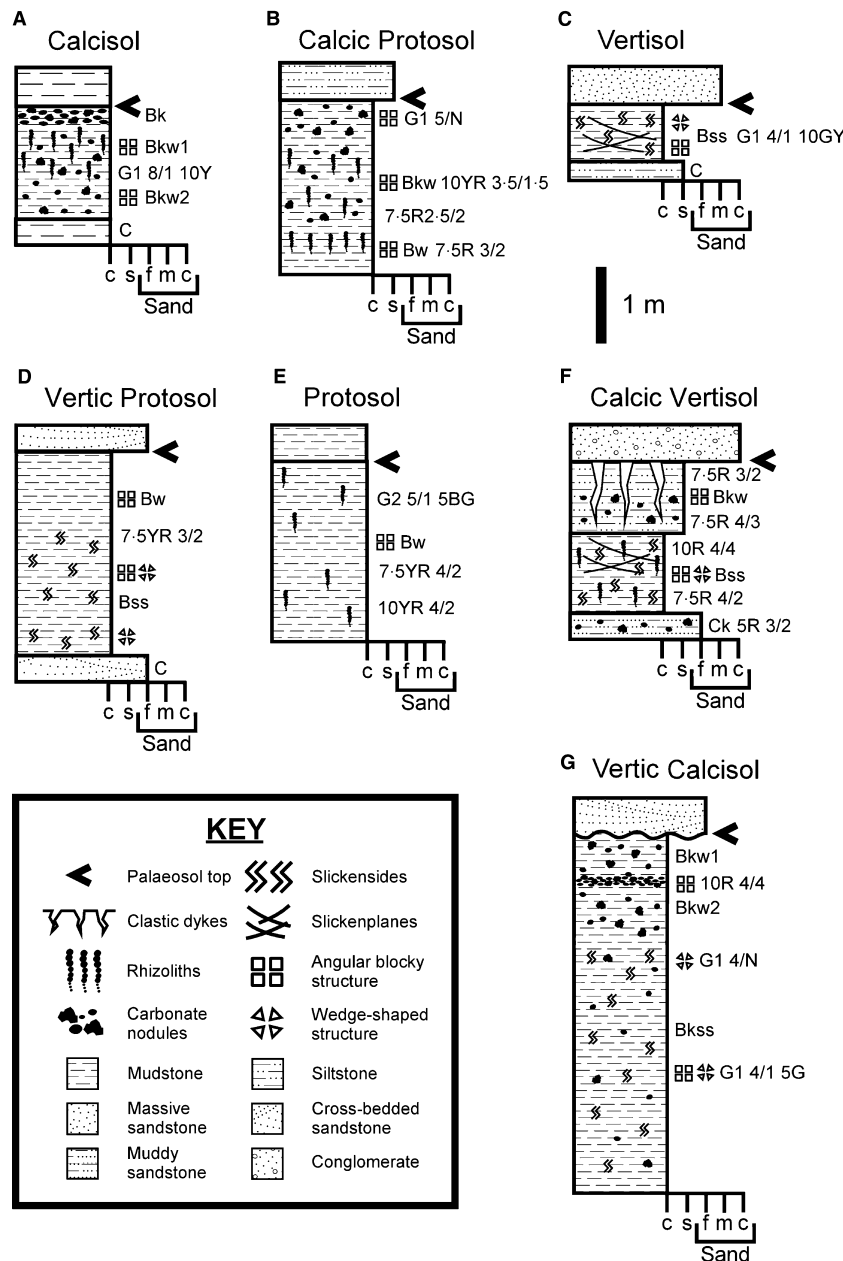


Fig. 6. Diagrammatic illustrations of representative palaeosol profiles described from the Lourinhã formation.

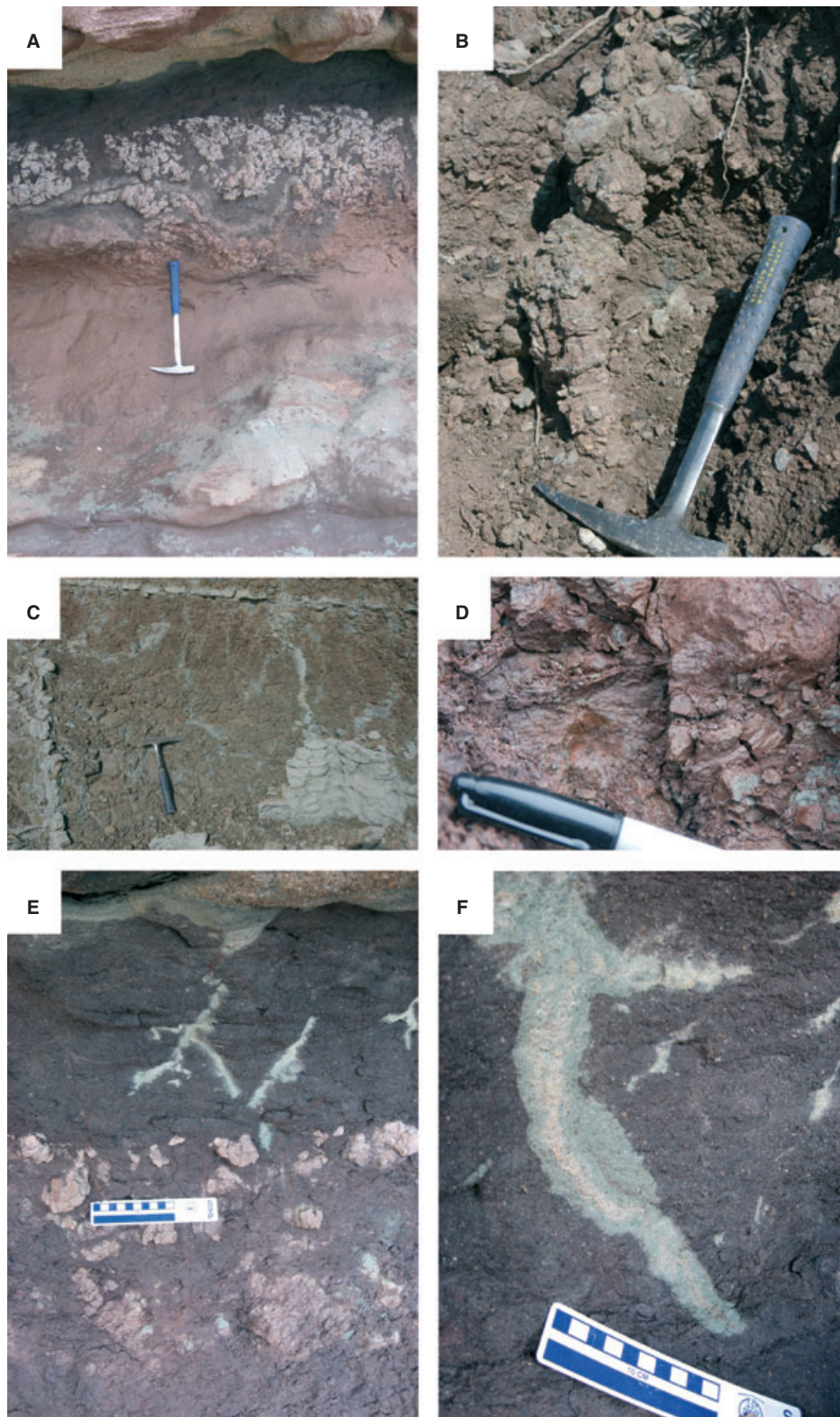


Fig. 7. Photographs of calcic and vertic features frequently observed in palaeosols of the Lourinhã formation: (A) carbonate nodules in stage II Bk horizon of a Calcisol (hammer for scale is 40.5 cm long); (B) calcareous rhizolith from a calcic Protosol (hammer for scale is 32.5 cm long); (C) large clastic dykes weathered out of a calcic Vertisol (hammer for scale is 32.5 cm long); (D) slickensides (part of pen for scale is 14 cm long); (E) clastic dykes and stage II Bk horizon in a vertic Calcisol; and (F) detailed view of clastic dyke from palaeosol shown in (E). Photographs (A), (E) and (F) are from the southern stratigraphic section and (B), (C) and (D) are from the northern section.

Table 1. Size terminology used in the text for pedogenic features.

	<1 cm	ca 1 cm	>1 cm
Nodules	Small	Medium	Large
Peds	Fine	Medium	Coarse
Mottles	Fine	Medium	Coarse
Slickensides	Small	Medium	Large

range from 0.5 to 5.0 m thick and are characterized by prominent calcic features, including abundant carbonate nodules and calcareous rhizoliths (Figs 6A and 7A). Carbonate nodules are typically small (see Table 1 for the size terminology used for pedogenic features) and may be either scattered throughout the profile or concentrated in thick Bk horizons. Occasionally, concentrated layers of nodules are cemented to form

stage III Bk horizons (*sensu* Gile *et al.*, 1966) up to 30 cm thick. Calcareous rhizoliths range from 2 to 6 cm in diameter, with an average diameter of approximately 4 cm; they are typically distributed throughout profiles, but may also be concentrated near the upper contact. Most Calcisol profiles show some evidence of gleying in the form of low chroma horizons or, more commonly, abundant grey or orange mottles ranging in size from fine to coarse (Fig. 8; Table 1). Lourinhã Calcisols developed in mudstones or silty mudstones commonly exhibit angular blocky structure, but profiles developed in coarser-grained deposits may be massive.

Calcic Protosols

Calcic Protosols are the dominant palaeosol type in the northern section, accounting for 44% of the described profiles. Twenty-three percent of palaeosol profiles in the southern section belong to this category, making it the second most abundant palaeosol type in that section. Profile thickness varies from 0.4 to 8.6 m, including several thick, cumulate profiles (*sensu* Marriott & Wright, 1993). Some Calcic Protosols preserve angular blocky ped structure, but soil structure in most profiles is typically poorly developed or altogether lacking, as is horizonation. Calcic Protosols are recognized by the presence of calcic features – typically sparsely distributed calcareous rhizoliths or carbonate nodules – in a profile with little or no horizonation (Figs 6B and 7B). Rhizoliths range from 1 to 7 cm in diameter, with an average of *ca* 4 cm. Carbonate nodules in these profiles are usually ≤ 1 cm in diameter, and they are not concentrated in prominent horizons as observed in Calcisol profiles. Slickensides and poorly developed wedge-shape ped structure occur rarely, but evidence of gleying is common, typically consisting of abundant fine to medium grey mottles (Fig. 8). These palaeosols usually develop in silty mudstones, and may also occur in fine-grained sandstone deposits.

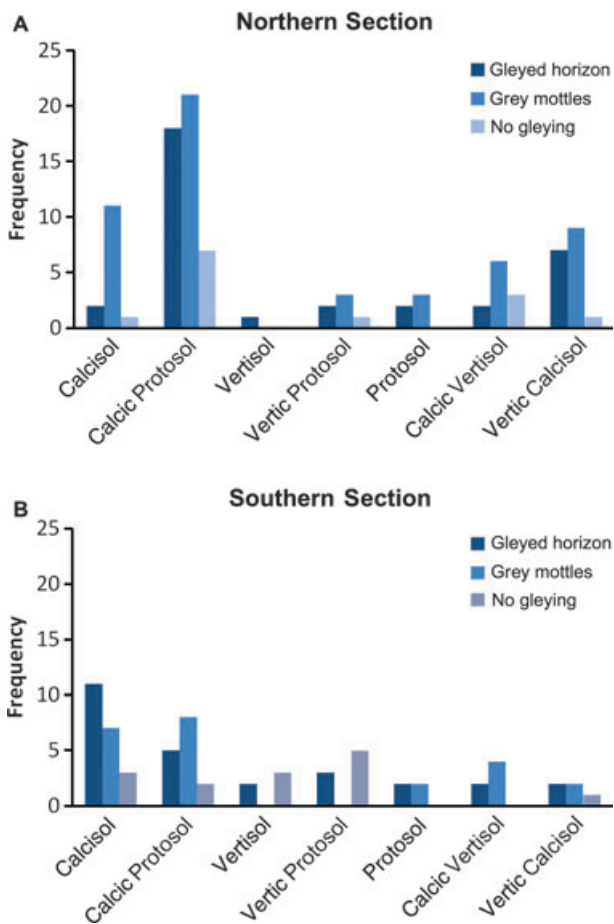


Fig. 8. Charts showing the abundance of gley features for each documented soil type: (A) northern; and (B) southern stratigraphic sections. Both stratigraphic sections are dominated by gley features, but relatively inconspicuous grey mottles are much more common in the northern section.

Vertisols

Vertisols occur rarely in the Lourinhã formation, accounting for 1% and 8% of the profiles in the northern and southern stratigraphic sections, respectively. These palaeosols range in thickness from 0.2 to 1.7 m, but rarely exceed 1.0 m. Lourinhã Vertisols are characterized by prominent vertic features such as common to abundant

slickensides and well-developed wedge-shaped structure (Fig. 6C). Peds range in size from fine to medium (Table 1). Slickensides are typically distributed throughout the profile, although they may also be concentrated in upper or lower horizons. Clastic dykes and slickenplanes are observed infrequently, and carbonate deposits are absent. When present, sandstone clastic dykes penetrate approximately 25 cm beneath the profile upper contact. All Lourinhã Vertisols formed in fine-grained mud-rich deposits and some, but not all, developed in greenish-grey, gleyed mudstones (Fig. 8). Mottles are not present in the described Vertisol profiles.

Vertic Protosols

Vertic Protosols are a relatively minor stratigraphic component of the Lourinhã formation, accounting for 6% and 13% of the palaeosol profiles in the northern and southern sections, respectively. Profile thicknesses range from 0.2 to 2.7 m and are generally less than 1.5 m. These palaeosols are characterized by large (>1 cm) slickensides that are distributed sparsely throughout the profile. Profiles typically display either massive structure or poorly developed wedge-shaped ped structure, with peds ranging in size from fine to coarse (Fig. 6D; Table 1). Clastic dykes composed of fine-grained sandstone extend downward from the profile upper contact and penetrate to depths between 25 cm and 80 cm. Matrix colour may be either grey or reddish (Fig. 8), but all profiles are devoid of carbonate. Mottling is observed infrequently in vertic Protosol profiles, but typically consists of abundant, fine to coarse grey mottles.

Protosols

This palaeosol type is distinguished by little more than basic angular blocky ped structure or non-calcareous root traces (Fig. 6E). Very few of the palaeosols in either the northern or southern sections (6%) may be classified as Protosols. Profiles range from 0.3 to 2.3 m in thickness, with most greater than 1.0 m. Ped structure is typically weakly developed, with an average ped size of *ca* 1 cm. Root traces may be distributed evenly throughout the profile, or they may increase in abundance upwards through the profile, forming a concentrated layer along the upper contact. These Protosols lack the vertic or calcic features observed in other palaeosol types in the Lourinhã formation. All Protosols possess either a gleyed

horizon or a mottled horizon, typically characterized by common, fine grey mottles (Fig. 8). Protosol profiles occur in either mudstones or fine-grained sandstones.

Calcic Vertisols

Eleven percent of the palaeosol profiles described in the northern section are classified as calcic Vertisols, and they compose 9% of the profiles in the southern section. Profiles are typically *ca* 2.0 m thick, but may reach thicknesses greater than 4.0 m due to cumulate processes (*sensu* Marriott & Wright, 1993). These palaeosols almost always possess clastic dykes along their upper contact (Figs 6F and 7C). The clastic dykes are composed of fine-grained sandstone and may extend up to 180 cm below the upper contact of the profile. Slickensides may or may not be present (Fig. 7D), and ped structure varies from wedge-shaped to angular blocky. Slickensides are typically large (Table 1) and are concentrated most often in the upper portion of the profile. Typically, ped structure is found throughout the profile, and peds range in size from fine to coarse, with fine to medium peds occurring most frequently. Carbonate features such as calcite nodules or calcareous rhizoliths are present, but are neither prominent nor abundant. Carbonate nodules range in size from small to large (Table 1), often increasing in both size and abundance upward in the profile. Calcareous rhizoliths range from 1 to 4 cm in diameter, with an average of approximately 2 cm. When present, rhizoliths are more common in the lower portion of the profile. Most calcic Vertisol profiles are characterized by either gleyed horizons or, more commonly, grey mottles; only 18% of Lourinhã calcic Vertisols lacks evidence of gleying (Fig. 8). Mottles are typically abundant, ranging in size from fine to medium, and may either increase or decrease in density through the profile. This palaeosol type forms only in fine-grained mudstone deposits.

Vertic Calcisols

This palaeosol type is the second most abundant palaeosol type in the northern section, composing 17% of the described profiles. In contrast, vertic Calcisols account for only 8% of the profiles in the southern section. Profile thicknesses range from 0.6 to 3.6 m, with compound sets of profiles (*sensu* Marriott & Wright, 1993) not uncommon. Characteristic attributes

of Lourinhã vertic Calcisols include prominent calcic features, such as concentrations of calcareous nodules and abundant calcareous rhizoliths (Figs 6G and 7E). Calcareous nodules range in size from small to large, but small nodules are much more common. When not dispersed throughout the profile, calcareous nodules typically increase in size and abundance moving upwards within the profile. Rhizoliths range from 1 to 6 cm in diameter, with an average of approximately 4 cm. Profiles may also contain cemented stage III Bk horizons (Gile *et al.*, 1966), ranging from 5 to 30 cm in thickness, and horizons defined by concentrations of discrete carbonate nodules commonly occur in the lower portions of profiles. Vertic features – including slickensides, and rarely clastic dykes or slickenplanes – are present, but less evident than calcic features (Fig. 7F). Slickensides typically occur throughout the profiles, but in some cases are confined to discrete upper or lower horizons within the profile. Ped structure may be either angular blocky or wedge-shape, with individual peds ranging in size from fine to medium. When present, clastic dykes composed of sandstone extend from the profile upper contact to depths up to 70 cm. In profiles where changes in ped structure are discernable, ped size generally increases upwards through the profile. Profiles with gley features are almost evenly split between those with gleyed horizons and those containing grey mottles (Fig. 8). Mottles, which typically increase in density downwards in the profile, are most often abundant and fine to coarse. Vertic Calcisols in the Lourinhã formation do not form in units coarser than silty mudstone.

Stratigraphic and spatial trends in palaeosol character

Pedogenically modified sediments compose a greater portion of the overall thickness of the northern section (45%) compared with the southern section (28%). Palaeosol profiles in the northern section are thicker and more poorly developed, as indicated by the abundance of Protosols. The southern section contains a similar density of palaeosols in terms of number of profiles per measured metre (Table 2), but these profiles are typically thin and compose a much smaller amount of the section by total thickness. Protosols are less common in the southern section, with Calcisols and Vertisols forming the majority of observed palaeosols.

Table 2. Abundances of palaeosol types within the northern and southern stratigraphic sections of the Lourinhã formation.

Palaeosol type	# of profiles	% of profiles	% of section thickness
Northern Section			
Calcisol	14	14	5
Calcic Protosol	45	45	21
Vertisol	1	1	<1
Vertic Protosol	6	6	2
Protosol	6	6	2
Calcic Vertisol	11	11	5
Vertic Calcisol	17	17	10
Southern Section			
Calcisol	21	33	7
Calcic Protosol	15	23	8
Vertisol	5	8	1
Vertic Protosol	8	13	2
Protosol	4	6	2
Calcic Vertisol	6	9	5
Vertic Calcisol	5	8	3

Within the northern section, palaeosol density is constant, and calcic and vertic features are distributed evenly throughout the sequence. However, Vertisols are concentrated between 80 m and 130 m. In addition, greater maturity of calcic palaeosols is evident in the middle of the section between 130 m and 255 m, with the development of several Calcisol profiles with stages II and III carbonate accumulations (*sensu* Gile *et al.*, 1966). In the southern section, palaeosol density increases in the upper third of the sequence. Calcic features also increase in abundance in the upper part of the section. Gley features are common in both sections, although the southern section contains more gleyed horizons compared with the northern section, in which less conspicuous mottling is the more common expression of gleying (Fig. 8).

Palaeosol profiles stratigraphically adjacent to the marine beds in both sections are primarily weakly developed Protosols. Strata overlying the marine units are typically not pedogenically modified, but beds directly beneath the shell lags may be either Protosols or Calcisols. In one instance, a transitional unit beneath a shell lag shows evidence of both marine and pedogenic influence. This bed is classified as a Protosol, based on the presence of weak angular blocky ped structure, and indicates temporary subaerial exposure and pedogenic overprinting of a near-shore marine deposit. In the southern section, Calcisols occur several metres above marine layers in two locations.

Table 3. X-ray fluorescence data and mean annual precipitation values ($n = 32$) calculated using the CIA-K index and equation from Sheldon *et al.* (2002). All CIA-K values are corrected for CaO derived from calcium carbonate. Average mean annual precipitation (MAP) is 1083 ± 178 mm/year (1σ).

Sample	Palaeosol type	wt% Al ₂ O ₃	wt% CaO	wt% Na ₂ O	CIA-K	MAP
PL003	Vertic Protosol	19.78	0.47	1.06	89	1266
PL023	Vertic Calcisol	16.83	0.57	1.37	84	1150
PL032	Vertic Protosol	19.99	0.33	1.17	89	1272
PL037	Vertisol	20.32	0.38	1.20	88	1261
PL040	Vertisol	19.86	0.41	1.17	88	1257
PL042	Calcic Protosol	15.12	8.74	1.26	76	993
PL062	Vertisol	19.99	0.36	0.75	91	1337
PL066	Calcic Vertisol	19.18	3.50	0.46	79	1045
PL074	Calcic Protosol	15.69	10.66	0.68	72	916
PL076	Calcic Protosol	17.05	7.80	0.62	89	1272
PL110	Calcic Vertisol	19.70	3.46	0.78	80	1079
PL116	Calcic Protosol	19.98	7.59	0.49	70	877
PL131	Calcic Vertisol	15.30	8.63	0.84	72	911
PL132	Calcic Vertisol	21.65	0.75	0.71	92	1360
PL135	Calcic Protosol	15.72	10.44	0.98	91	1323
PT019	Calcic Protosol	17.58	8.15	0.38	68	835
PT024	Calcic Vertisol	15.73	8.37	0.66	72	908
PT033	Calcic Protosol	18.12	6.68	0.49	74	953
PT040	Calcic Protosol	21.00	3.62	0.49	80	1058
PT057	Calcic Protosol	18.25	6.24	0.24	69	868
PT092	Calcic Protosol	16.93	5.54	0.65	78	1031
PT098	Calcic Protosol	17.78	4.13	0.59	94	1394
PT101	Vertisol	21.65	2.30	0.46	86	1193
PT113	Calcic Protosol	18.10	5.10	0.55	71	897
PT124	Calcic Protosol	18.25	5.36	0.35	74	953
PT136	Calcic Protosol	19.62	3.82	0.49	84	1152
PT147	Calcic Protosol	17.53	8.01	0.72	63	766
PT150	Calcic Vertisol	17.64	6.31	0.91	75	962
PT164	Calcic Protosol	17.73	4.60	0.92	72	905
PT169	Calcic Protosol	21.48	1.56	0.93	87	1236
PT178	Calcic Protosol	17.94	0.89	1.73	85	1169
PT187	Calcic Protosol	17.11	3.41	1.42	80	1071

Major-element chemistry of palaeosol B-horizons

Elemental data for the 32 samples selected for XRF analysis are summarized in Table 3; only oxides used for calculation of the chemical index of alteration minus potassium are shown. Weight percent Al₂O₃ in all samples varies between 15.1 and 21.7%. CaO and Na₂O range from 0.3 to 10.7% and 0.2 to 1.7%, respectively. Chemical index of alteration minus potassium (CIA-K) values were calculated using the original function of Nesbitt & Young (1982) with K₂O removed (Maynard, 1992):

$$\text{CIA} - \text{K} = \frac{\text{Al}_2\text{O}_3}{\text{Al}_2\text{O}_3 + \text{CaO} + \text{Na}_2\text{O}} * 100 \quad (1)$$

Al₂O₃, CaO and Na₂O are molar proportions calculated for each sample. Weight percent car-

bonate was measured for each sample, and all CIA-K values were corrected by subtracting the moles of CaO derived from calcium carbonate from the total measured CaO. Calculated CIA-K values range between 63 and 94, with an average of 80. When the two measured sections of the Lourinhã formation are compared, the northern section has a slightly larger range of CIA-K values ($n = 17$, range = 63–94, average = 77), but produces an average index similar to that of the southern section ($n = 15$, range = 70–92, average = 83).

X-ray diffraction – analysis of clay minerals

The mineralogy of two clay-rich samples from representative Vertisol profiles, one from each measured section, is summarized in Fig. 9. The total clay fraction of each sample contains variable amounts of smectite, illite and kaolinite,

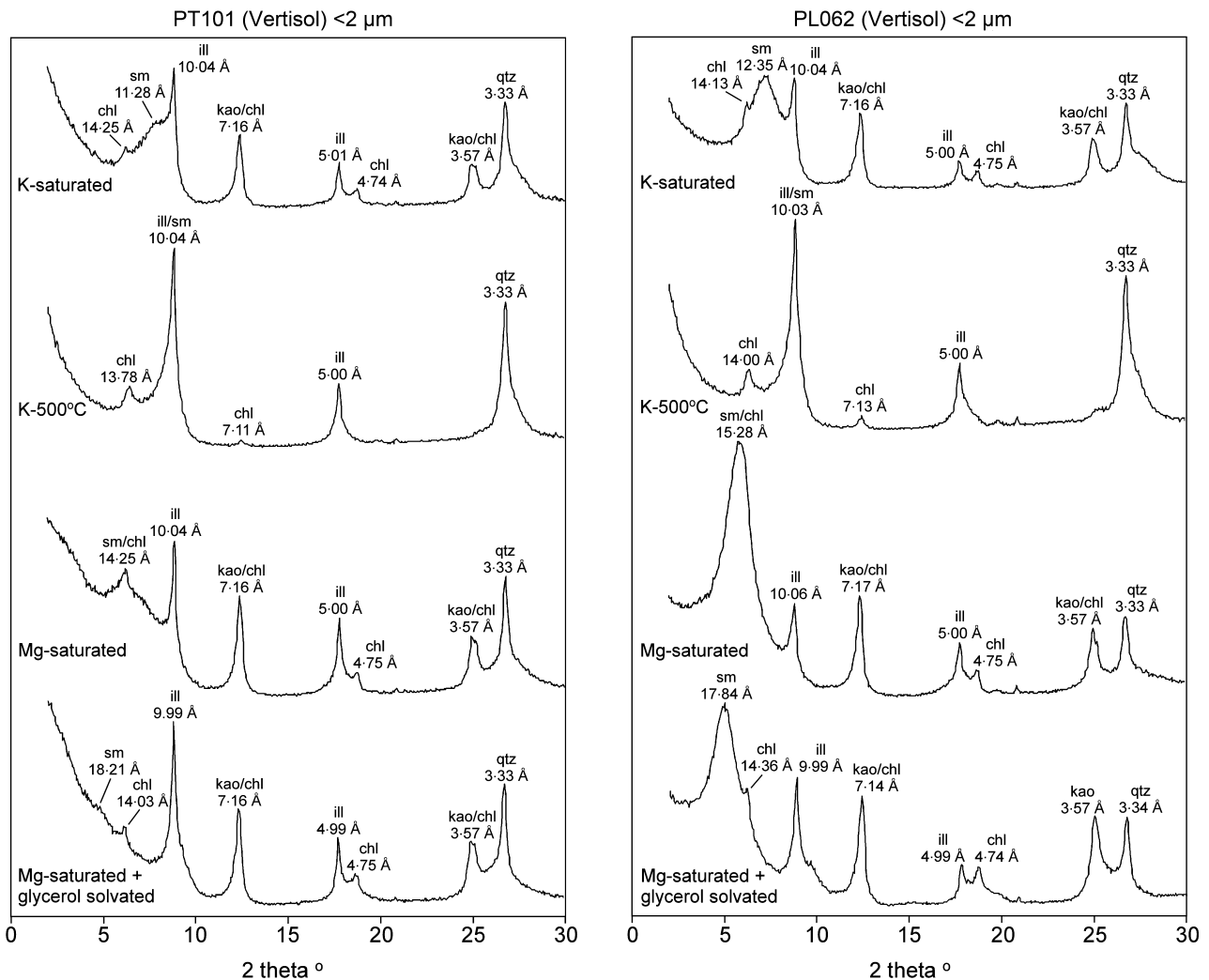


Fig. 9. XRD spectra for oriented aggregates of the total clay fraction (<2 μm) from two Vertisols. Both Vertisols contain a mixture of illite, smectite, kaolinite and chlorite. The Vertisol from the southern stratigraphic section (PL062, 127 m) has a higher percentage of smectite than the Vertisol from the northern section (PT101, 176 m).

with trace amounts of chlorite. Sample PT101, collected from the northern section, contains an abundance of illite and kaolinite, but only small amounts of smectite in the <2 μm fraction. In contrast, sample PL062 from the southern section is dominated by smectite, with only minor contributions from illite and kaolinite in the <2 μm fraction. Although there is considerable variability in the relative abundance of smectite, illite and kaolinite within each section, some broad trends are apparent. In the northern section, kaolinite averages about 30% of the total clay fraction. Illite typically accounts for around half of the clay mineral assemblage, with smectite composing the remainder (Fig. 10A). The southern section shows more variability in the relative abundance of these three mineral constituents

(Fig. 10B). Kaolinite still composes around 30% of the total clay fraction on average, but there is a larger average proportion of smectite relative to illite. The lower half of the southern section, in particular, has a higher abundance of smectite. The relative proportions of clay minerals in the northern section remain virtually constant, with slight increases in smectite near the top and bottom of the section.

Comparison of the total clay fraction (<2 μm) with the fine clay fraction (<0.2 μm) reveals similar overall trends in relative mineralogical abundance with only minor differences. Fine clay assemblages from the northern section are still dominated by illite and kaolinite, with minimal contributions from smectite (Fig. 11A). There is a slight reduction in the average abundance of

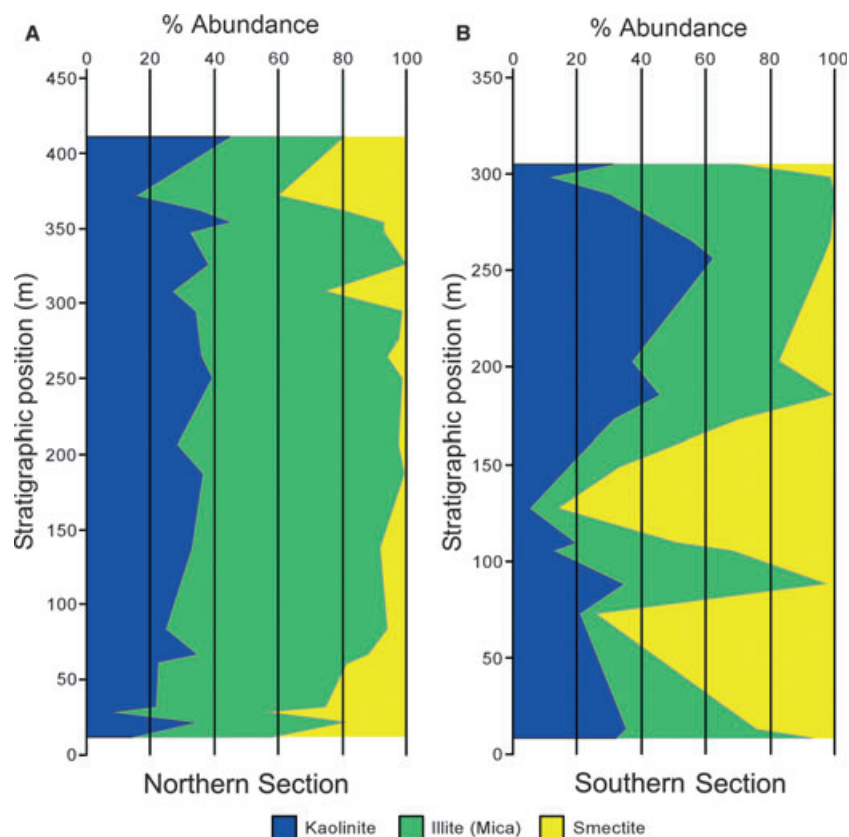


Fig. 10. Relative abundance of clay minerals in palaeosols from the northern and southern stratigraphic sections of the Lourinhã formation (total clay fraction, $<2 \mu\text{m}$). The northern section has a lower abundance of smectite relative to the southern section, where smectitic clays are concentrated in the lower half of the section.

smectite, from 15% to less than 10%, relative to the total clay fraction. The relative abundance of minerals in the fine clay fractions from the southern section is also broadly similar to that observed in the total clay assemblage. Fine clay sample fractions from the lower part of the southern section are dominated by smectite (Fig. 11B), in contrast to the general lack of smectite observed in samples from the northern section.

Oxygen-isotope and hydrogen-isotope analyses of clay minerals

The $\delta^{18}\text{O}$ and δD values measured from three fine clay sample fractions of selected palaeosol B-horizons are listed in Table 4. The $\delta^{18}\text{O}$ values are similar, ranging from $+22.4$ to $+22.7\text{‰}$ SMOW, but the δD values show greater variability, with a range of -53.0 to -37.3‰ SMOW. The sample with the lowest δD value was collected from the southern section, and the other two samples are from palaeosol profiles in the northern section.

DATA INTERPRETATION AND DISCUSSION

Late Jurassic climate of Portugal

The stratigraphic distribution of palaeosols within the two measured sections indicates little change in palaeoclimate conditions during the time in which the majority of the Lourinhã formation was deposited. The abundance of Calcisols and Vertisols in both sections suggests that local conditions were characterized by a highly seasonal rainfall distribution, as previously suggested by Hill (1989). Modern Calcisols form primarily in the dry tropical, dry sub-tropical and wet-dry tropical zones between 15° and 30° north and south latitude that are characterized by soil-forming environments with net moisture deficits (Mack & James, 1994; Birkeland, 1999). Although abundant pedogenic carbonate accumulations often indicate arid conditions with mean annual precipitation less than 760 mm/year (Royer, 1999), pedogenic carbonate may be retained in environments with mean annual precipitation ranging

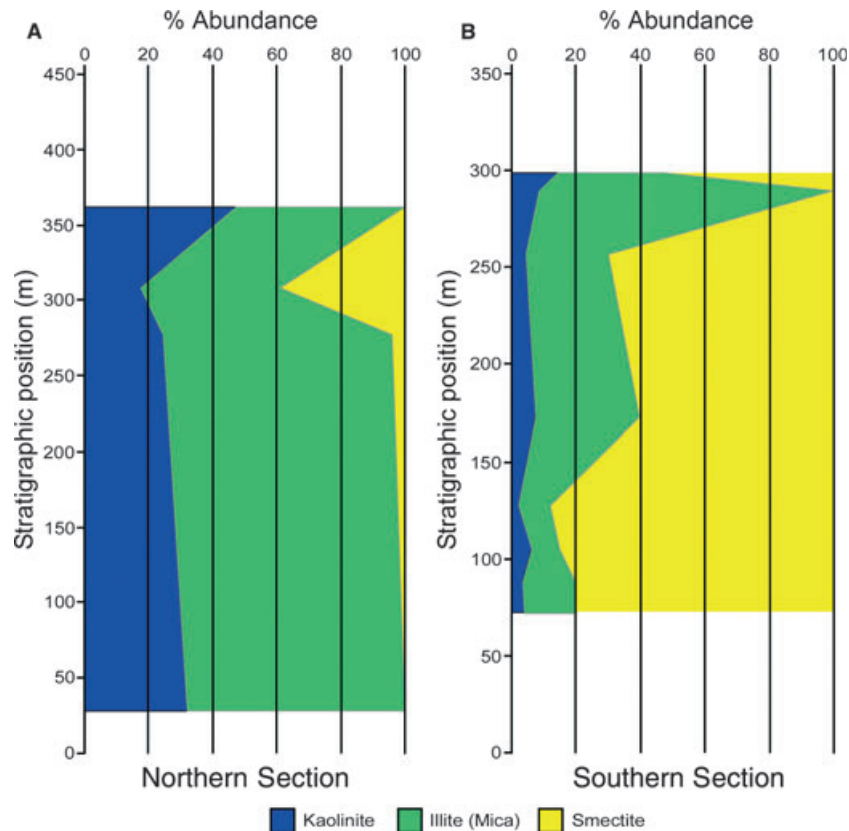


Fig. 11. Relative abundance of clay minerals in palaeosols from the northern and southern stratigraphic sections of the Lourinhã formation (fine clay fraction, $<0.2 \mu\text{m}$). Basic trends mirror those observed in the total clay fraction, but the abundance of smectite in the southern section is greater.

from 600 to 1000 mm/year, depending on local environmental factors (Mack & James, 1994). Vertisols, in particular, may retain pedogenic carbonate in environments with rainfall greater than 1400 mm/year, due to their high clay content and consequently low permeability (Nordt *et al.*, 2006). Vertic features, created by shrink and swell processes resulting from cyclical wetting and drying, are typical of environments with pronounced seasonality of rainfall (Wilding & Tessier, 1988; Coulombe *et al.*, 1996). Therefore, the pedogenic carbonates found throughout the Lourinhã formation are interpreted as evidence of strongly seasonal precipitation rather than overall

arid conditions. These general climatic interpretations based on palaeosol morphology are corroborated by analysis of clay minerals.

The increase in abundance of smectite between the total and fine clay fractions in the southern section implies that much of the kaolinite and illite is detrital, whereas the smectite component is largely of pedogenic origin. The presence of smectite in the total and fine clay fractions of many Lourinhã palaeosols is consistent with the observed prevalence of vertic features. Authigenic smectite typically forms in dry environments with minimal chemical weathering (Singer, 1984; Curtis, 1990), although smectite

Table 4. Measured $\delta^{18}\text{O}$ and δD values and calculated mean annual palaeotemperature estimates from pedogenic clay minerals in the Lourinhã formation. Temperature values should be considered maximum estimates due to errors resulting from variable sample composition. mab = metres above base.

Sample	Stratigraphic position (mab)	Palaeosol type	Section	$\delta^{18}\text{O}$ (‰SMOW)	δD (‰SMOW)	Temperature ($^{\circ}\text{C}$) $\pm 3^{\circ}$
PT024	29	Calcic Vertisol	Northern	+22.7	-37.3	39
PT101	276	Vertisol	Northern	+22.5	-44.2	36
PL062	127	Vertisol	Southern	+22.4	-53.0	32

may also develop under humid conditions (Singer, 1984), or as a result of poor drainage that leads to incomplete leaching of the soil profile. The occurrence of kaolinite throughout Lourinhã fine clay assemblages, albeit in small amounts, suggests that soil development occurred under relatively moist conditions because kaolinite is indicative of wet environments with high rates of chemical weathering (Keller, 1970; Singer, 1984). The greater abundance of kaolinite in the fine clay fraction of the northern section may be the result of greater landscape stability (longer intervals between depositional or erosional events), as reflected by the lower ratio of Protosols to other soil orders (0.75) relative to the southern section (1.0), or better drainage of soil profiles.

Estimates of mean annual palaeoprecipitation were calculated using the mathematical relationship between MAP and CIA-K values reported by Sheldon *et al.* (2002):

$$\text{MAP}(\text{mm/year}) = 221e^{0.0197(\text{CIA-K})} \quad (2)$$

This method of estimating precipitation was used instead of the depth to carbonate proxy (Retallack, 1994) because the original soil surface was often difficult to identify in the cumulate and

composite palaeosol profiles that occur frequently in the Lourinhã sections. Precipitation estimates vary with time through both the northern and southern sections and also vary according to soil type (Table 3). Annual rainfall estimates from the northern section range from 766 mm/year to 1394 mm/year. Northern Protosols and Vertisols show a similar trend of slightly increasing palaeoprecipitation through the section (Fig. 12). Estimates from the southern section range from 877 mm/year to 1360 mm/year. Protosols and Vertisols again show similar trends in CIA-K values and corresponding palaeo-rainfall estimates, but southern palaeosols record decreasing palaeoprecipitation estimates moving upsection, in contrast to results from the northern section. The overall average mean annual precipitation estimate for the Lourinhã formation is 1100 mm/year ($n = 32$, $1\sigma = 178$), with mean values of 1021 ± 165 mm/year (1σ) and 1155 ± 169 mm/year (1σ) for the northern and southern sections, respectively.

The average MAP estimates derived from XRF analyses for the northern (1021 mm/year) and southern (1155 mm/year) sections are higher than might be expected given the prevalence of calcic features in the Lourinhã formation. However, these MAP estimates are similar to the approxi-

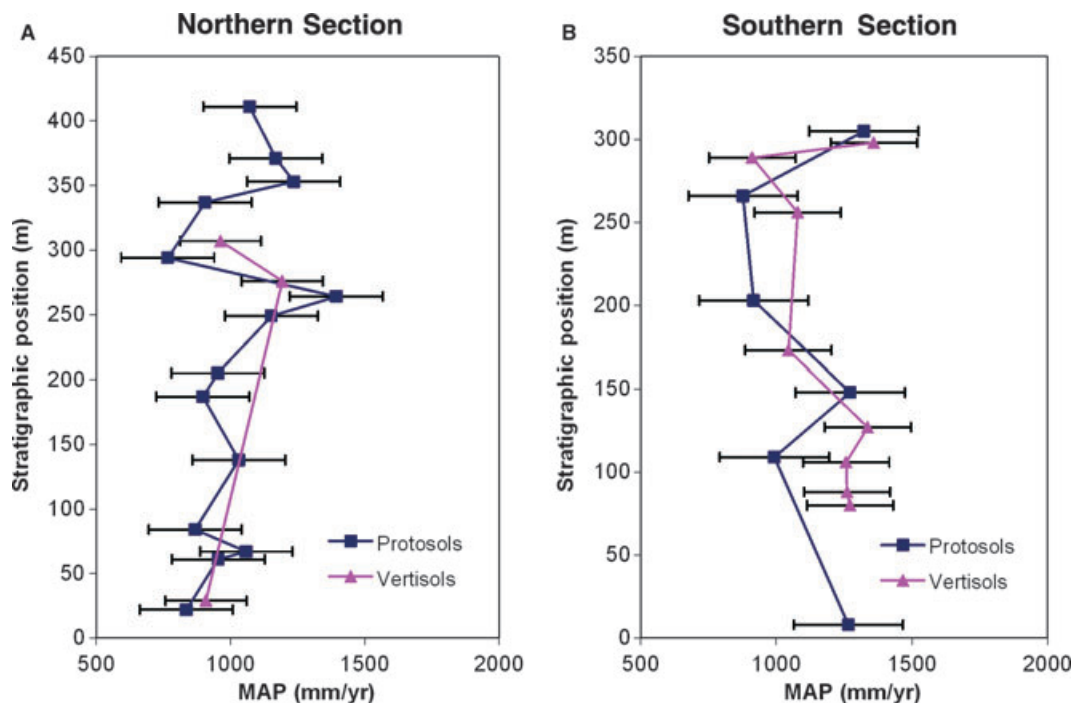


Fig. 12. Mean annual precipitation (MAP) estimates for Protosols and Vertisols from the northern and southern stratigraphic sections of the Lourinhã formation. Estimates for samples from the northern section show a pattern of slightly increasing MAP through time, whereas samples from the southern section suggest decreasing or invariant MAP. Error bars represent 1σ .

mately 1100 mm/year estimate produced for Late Jurassic Iberia by a recent general circulation model (GCM) simulation (Sellwood & Valdes, 2008, fig. 5a). The average MAP value of 1100 mm/year estimated here for the Lourinhã formation is not incompatible with the observed abundance of pedogenic carbonates because, as noted previously, soils rich in clays may retain pedogenic carbonate under conditions where average annual precipitation exceeds 1400 mm/year (Nordt *et al.*, 2006). Presence of roughly contemporaneous Kimmeridgian coal deposits at Guimarota 75 km north-east of Lourinhã (Helmdach, 1971; Schudack, 2000) also implies that regional conditions were characterized by high annual rainfall and relative humidity. However, the Guimarota coal measures developed near sea-level under at least periodic marine influence (Helmdach, 1971), and coal accumulation at that site may reflect influence of shallow ground water rather than significant precipitation.

Palaeotemperature estimates for the Lourinhã formation were calculated using the $\delta^{18}\text{O}$ and δD values of the fine clay fraction sampled from palaeosol B-horizons. This approach utilizes the equation derived by Delgado & Reyes (1996), rearranged to isolate the temperature variable:

$$T_{\text{K}} = \sqrt{\frac{3.54 \times 10^6}{\delta^{18}\text{O} - 0.125\delta\text{D} + 8.95}} \quad (3)$$

Three samples yield $\delta^{18}\text{O}$ and δD values that correspond to palaeotemperature estimates ranging

from 32 to 39°C \pm 3° (Table 4), with an average of 36°C. The clay minerals used in this analysis are assumed to have formed in isotopic equilibrium with meteoric waters (Fig. 13). If the isotopic composition of Lourinhã surface waters was influenced by intense evaporation, the function describing the $\delta^{18}\text{O}$ and δD values would plot to the right of the meteoric water line (Savin & Hsieh, 1998). As a result, the measured isotopic values of the clay minerals formed in the presence of heavily evaporated waters would indicate palaeotemperatures even higher than the estimates reported here. However, given the lack of sedimentary evidence for severe evaporative conditions during deposition of the Lourinhã formation, the palaeotemperature estimates are unlikely to have been affected by this type of enrichment fractionation.

The composition of the clay mineral samples used in this analysis is another source of potential error. The temperature equation presented by Delgado & Reyes (1996) was derived for smectite, and the samples analyzed here contain variable amounts of kaolinite and illite in addition to smectite. The equations describing the temperature dependence of the oxygen and hydrogen fractionation factors for kaolinite and mixed-layer illite-smectite differ from those for smectite (Capuano, 1992; Savin & Hsieh, 1998), such that the temperature estimates presented here should be considered maximum values of soil temperature at the time of phyllosilicate crystallization.

The soil palaeotemperatures derived here from clay minerals are affected by variable sample composition, but still constrain maximum estimates of

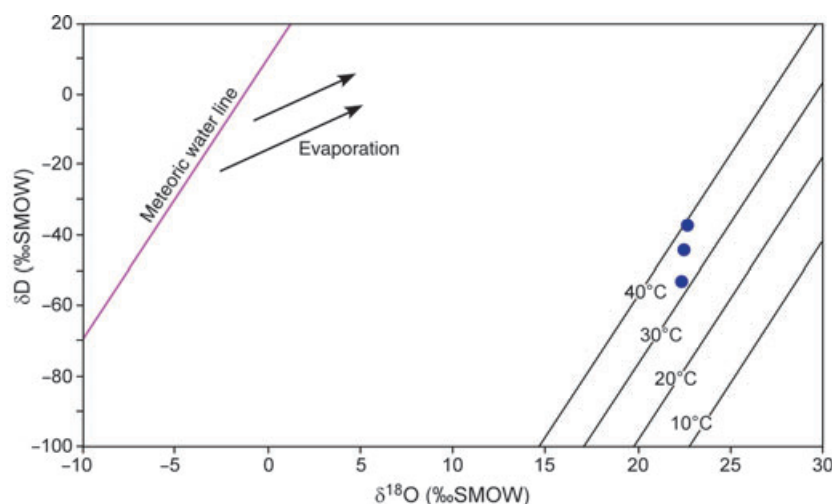


Fig. 13. Plot of $\delta^{18}\text{O}$ versus δD values for pedogenic clay mineral samples from palaeosol B-horizons in the Lourinhã formation. The meteoric water line is shown at the left, and the isotherms on the right represent potential compositions of smectite formed in equilibrium with meteoric waters at different temperatures. The measured isotopic compositions of the three samples suggest an upper limit for soil palaeotemperature between 32°C and 39°C.

soil temperature. In modern soil-forming environments, average annual soil temperatures are typically higher than mean annual air temperatures in both high and low latitude settings (Dedecek *et al.*, 2006; Passey *et al.*, 2010). The difference between soil and air temperature is dependent upon a number of factors, including vegetation cover, snow cover and soil moisture (Zhang *et al.*, 2005). Given the warmer soil temperature estimates produced here, a soil–air temperature offset of 5°C, measured in warm low latitude modern environments (Passey *et al.*, 2010) is used. Applying this 5°C offset, the soil temperatures estimated here for the Lourinhã formation would correspond to surface temperatures between 27°C and 34°C, with a 31°C mean. These palaeotemperature values are similar to surface temperature estimates derived from GCM simulations of Late Jurassic climate. Modelled mean surface temperatures for Iberia in Northern Hemisphere summer months (June, July and August) range from *ca* 25°C (Valdes & Sellwood, 1992; Sellwood & Valdes, 2008) to 30°C (Rees *et al.*, 2000). General circulation model estimates of winter (December, January and February) temperatures are lower overall, but vary more between studies. An earlier analysis by Valdes & Sellwood (1992) produced estimates near 25°C, whereas the model used by Rees *et al.* (2000) calculates winter temperatures as low as 10°C, and a simulation by Sellwood & Valdes (2008) suggests an intermediate temperature of *ca* 15°C. Given that the palaeotemperature estimates from this study are closer to the warm summer temperatures generated by GCM simulations, Late Jurassic Iberia may have been a few degrees warmer than suggested by palaeoclimate models.

Comparison with the Western United States

The data presented here indicate that the Lourinhã formation was deposited under warm, sub-humid conditions, with a strongly seasonal distribution of rainfall. Recent studies of the Morrison Formation suggest a broadly similar type of palaeoclimate. Sedimentary facies strongly linked to semi-arid climate, such as those developed in playas and saline lakes, constitute a major part of the Morrison Formation (Turner & Fishman, 1991; Demko & Parrish, 1998). Observations of palaeosol morphology and distribution within the Morrison Formation suggest a semi-arid to tropical wet–dry climate with some degree of seasonality in precipitation (Demko *et al.*, 2004). Conditions in the western and southern areas of deposition are proposed

to be drier and, over the entire formation, there is a stratigraphic trend of palaeoclimate indicators that suggests increasing humidity through time (Demko *et al.*, 2004). Study of palustrine and lacustrine carbonates in the Morrison Formation also indicates a semi-arid climate with little rainfall and ground water as the primary source of water in moist sub-environments (Dunagan & Turner, 2004). Plant remains from the Morrison Formation are consistent with a warm, semi-arid, seasonal climate as well (Parrish *et al.*, 2004), and seasonal rainfall in some parts of the Morrison ecosystem is reinforced by analysis of growth bands in bivalves (Good, 2004). Coal beds up to 3 m thick are present in the Morrison Formation in west-central Montana (Silverman & Harris, 1967; Daniel *et al.*, 1992). Located within the higher latitudes of the Morrison depositional area, these coal deposits are thought to have formed under seasonally dry conditions, preserved by a perennially high water table (Demko *et al.*, 2004). Abundant fusain and inert coals comprising heavily oxidized plant material are attributed to seasonally recurring wildfires within the local palustrine environments (Daniel *et al.*, 1992).

The Lourinhã and Morrison formations were deposited at roughly equivalent palaeolatitudes (Smith *et al.*, 1994), although the Morrison Formation occupied a larger geographic area and spanned a greater latitudinal interval (approximately 30 to 40°N). The greatest difference in these two formations is their proximity to the ocean. On the Colorado Plateau, basal parts of the Morrison Formation developed in marginal marine environments near the edge of a retreating epicontinental sea (O’Sullivan, 1992; Peterson, 1994), but the bulk of the formation was deposited in fully terrestrial environments in the centre of the North American continent (Turner & Peterson, 2004). In contrast, the Lourinhã formation was deposited on the isolated, Iberian landmass in close proximity to an epicontinental embayment of the recently opened North Atlantic (Pena dos Reis *et al.*, 2000), and both the Lourinhã formation and the nearby Guimarota beds show evidence of marine influence (Fürsich, 1981; Gloy, 2000; Kriwet, 2000). Preservation of both the Guimarota and Morrison coals was probably facilitated by the presence of shallow ground water, but the presence of well-developed palustrine palaeoenvironments without evidence of seasonality at Guimarota nonetheless implies wetter conditions and higher overall precipitation

relative to the coal-forming environments of the Morrison Formation.

The Morrison and Lourinhã formations both contain palaeosols with indicators of seasonal precipitation and moisture deficit, but MAP estimates suggest that Portuguese palaeoenvironments were characterized by higher annual rainfall. Contemporaneous coal deposits are present within the same structural basin as the Lourinhã formation, while the coal beds in the Morrison Formation are well-developed only in northern strata deposited in closer proximity to the retreating epicontinental sea. Beginning in the Middle Jurassic, the splintering of Western Europe into a number of relatively small landmasses, divided at least periodically by shallow epicontinental seaways (Upchurch *et al.*, 2002), imposed a coastal marine climate regime that differed from the more arid continental climate of the North American interior where the Morrison ecosystem developed.

CONCLUSIONS

The Late Jurassic palaeoclimate of Portugal was warm and sub-humid with a strongly seasonal pattern of precipitation. Maximum estimates of soil temperature derived from isotopic analysis of clay minerals correspond to surface temperatures between 27°C and 34°C, with an average of 31°C. These estimates are similar to summer surface temperature estimates generated by general circulation model (GCM) palaeoclimate simulations for Late Jurassic Iberia, but suggest temperatures at least 1°C higher, on average, than the highest modelled estimates. A mean annual precipitation estimate of approximately 1100 mm/year, produced using the chemical index of alteration minus potassium geochemical climofunction, also compares favourably with GCM results. The abundance of pedogenic carbonates throughout the Lourinhã formation reflects seasonal precipitation rather than pronounced aridity. The retention of carbonate features under wetter conditions is attributed to the low permeability of the mud-rich Lourinhã deposits, which inhibits infiltration and percolation of water through the soil profiles. Seasonality of rainfall is reflected by the abundance of vertic features present in palaeosols throughout the Lourinhã formation.

The data presented here indicate that the Lourinhã formation was deposited under wetter, more humid palaeoclimatic conditions than the Morrison Formation. This difference in humidity

and mean annual precipitation is interpreted as a result of differing palaeogeographic settings. Lourinhã palaeoenvironments received more rainfall because they developed in a coastal marine setting adjacent to the proto-North Atlantic, whereas the Morrison Formation was deposited under drier continental interior conditions. The seasonal nature of moisture availability in both Morrison and Lourinhã palaeoenvironments does not appear to have impaired their ability to support a rich and abundant terrestrial fauna. Despite the inferred differences in annual precipitation between the Lourinhã and Morrison formations, their broadly similar warm and seasonal climate helps to explain the similarity of the terrestrial vertebrate faunas preserved in these Upper Jurassic deposits.

ACKNOWLEDGEMENTS

We thank Kurt Ferguson and Ian Richards in the Southern Methodist University (SMU) Stable Isotope Laboratory for their assistance with isotopic analyses. Kurt Ferguson, Karen Gutierrez, and Lauren Michel assisted with field work. Dale Winkler provided helpful, insightful comments on an earlier version of this manuscript. Constructive critical comments from reviewers Greg Ludvigson and Stephen Hesselbo and Associate Editor Adrian Immenhauser greatly improved the quality of this paper. This project was funded in part by the Roy M. Huffington Department of Earth Sciences at SMU and the Roy M. Huffington Graduate Fellowship. Research funding was also provided by grants awarded to the senior author by the Institute for the Study of Earth and Man, the Jurassic Foundation, the Western Interior Paleontological Society, the Paleontological Society and the Geological Society of America.

REFERENCES

- Alves, T.M., Gawthorpe, R.L., Hunt, D.W. and Monteiro, J.H. (2002) Jurassic tectono-sedimentary evolution of the Northern Lusitanian Basin (offshore Portugal). *Mar. Petrol. Geol.*, **19**, 727–754.
- Alves, T.M., Manuppella, G., Gawthorpe, R.L., Hunt, D.W. and Monteiro, J.H. (2003) The depositional evolution of diapir- and fault-bounded rift basins: examples from the Lusitanian Basin of West Iberia. *Sed. Geol.*, **162**, 273–303.
- Antunes, M.T. and Mateus, O. (2003) Dinosaurs of Portugal. *C. R. Palevol.*, **2**, 77–95.
- Azerêdo, A.C., Ramalho, M.M. and Wright, V.P. (1998) The Middle–Upper Jurassic disconformity in the Lusitanian

- Basin, Portugal: preliminary facies analysis and evidence for palaeoclimatic fluctuation. *Cuad. Geol. Ibér.*, **24**, 99–119.
- Azerêdo, A.C., Wright, V.P. and Ramalho, M.M.** (2002) The Middle-Late Jurassic forced regression and disconformity in central Portugal: eustatic, tectonic and climatic effects on a carbonate ramp system. *Sedimentology*, **49**, 1339–1370.
- Birkeland, P.W.** (1999) *Soils and Geomorphology*. Oxford University Press, New York, 430 pp.
- Capuano, R.M.** (1992) The temperature dependence of hydrogen isotope fractionation between clay minerals and water, evidence from a geopressed system. *Geochim. Cosmochim. Acta*, **56**, 2547–2554.
- Clayton, R.N. and Mayeda, T.K.** (1963) The use of bromine pentafluoride in the extraction of oxygen from oxides and silicates for isotopic analysis. *Geochim. Cosmochim. Acta*, **27**, 43–52.
- Coulombe, C.E., Dixon, J.B. and Wilding, L.P.** (1996) Mineralogy and chemistry of Vertisols. In: *Vertisols and Technologies for Their Management. Developments in Soil Science*, 24 (Eds N. Ahmad and A. Mermut), pp. 115–200. Elsevier, New York.
- Currie, B.S.** (1998) Upper Jurassic–Lower Cretaceous Morrison and Cedar Mountain formations, NE Utah–NW Colorado: relationships between nonmarine deposition and early Cordilleran foreland-basin development. *J. Sed. Res.*, **68**, 632–652.
- Curtis, C.D.** (1990) Aspects of climatic influence on the clay mineralogy and geochemistry of soils, palaeosols and clastic sedimentary rocks. *J. Geol. Soc. Lond.*, **147**, 351–357.
- Daniel, J.A., Bartholomew, M.J. and Murray, R.C.** (1992) Geological characteristics of the Stockett bed coal in the central Great Falls coal field, Montana. *M.T. Bur. Mines Geol. Spec. Publ.*, **102**, 145–157.
- Dedecek, P., Safanda, J., Kresl, M. and Cermak, V.** (2006) Ground surface temperature monitoring under different types of surfaces—the three year results. *Geophys. Res. Abstr.*, **8**, 07795.
- Delgado, A. and Reyes, E.** (1996) Oxygen and hydrogen isotope compositions in clay minerals: a potential single-mineral geothermometer. *Geochim. Cosmochim. Acta*, **60**, 4285–4289.
- Demko, T.M. and Parrish, J.T.** (1998) Paleoclimatic setting of the Upper Jurassic Morrison Formation. *Mod. Geol.*, **22**, 283–296.
- Demko, T.M., Currie, B.S. and Nicoll, K.A.** (2004) Regional paleoclimatic and stratigraphic implications of paleosols and fluvial/overbank architecture in the Morrison Formation (Upper Jurassic), Western Interior, USA. *Sed. Geol.*, **167**, 115–135.
- Dunagan, S.P.** (2000) Constraining Late Jurassic paleoclimate within the Morrison paleoecosystem: insights from the terrestrial carbonate record of the Morrison Formation (Colorado, USA). *Geores. Forum*, **6**, 523–532.
- Dunagan, S.P. and Turner, C.E.** (2004) Regional paleohydrologic and paleoclimatic settings of wetland/lacustrine depositional systems in the Morrison Formation (Upper Jurassic), Western Interior, USA. *Sed. Geol.*, **167**, 269–296.
- Foster, J.R.** (2003) Paleoeological analysis of the vertebrate fauna of the Morrison Formation (Upper Jurassic), Rocky Mountain Region, U.S.A. *N.M. Mus. Nat. Hist. Sci. Bull.*, **23**, 1–95.
- Fürsich, F.T.** (1981) Salinity-controlled benthic associations from the Upper Jurassic of Portugal. *Lethaia*, **14**, 203–223.
- Gile, L.H., Peterson, F.F. and Grossman, R.B.** (1966) Morphological and genetic sequences of carbonate accumulation in desert soils. *Soil Sci.*, **101**, 347–360.
- Gloy, U.** (2000) Taphonomy of the fossil lagerstätte Guimarota. In: *Guimarota: A Jurassic Ecosystem* (Eds T. Martin and B. Krebs), pp. 129–136. Verlag Dr. Friedrich Pfeil, Munich.
- Golonka, J.** (2007) Late Triassic and Early Jurassic palaeogeography of the world. *Palaeogeogr. Palaeoclimatol. Palaeoecol.*, **244**, 297–307.
- Golonka, J. and Ford, D.** (2000) Pangean (Late Carboniferous–Middle Jurassic) paleoenvironment and lithofacies. *Palaeogeogr. Palaeoclimatol. Palaeoecol.*, **161**, 1–34.
- Golonka, J., Edrich, M.E., Ford, D.W., Pauken, R.J., Bocharova, N.Y. and Scotese, C.R.** (1996) Jurassic paleogeographic maps of the world. In: *The Continental Jurassic* (Ed M. Morales), pp. 1–5. Museum of Northern Arizona, Flagstaff.
- Good, S.C.** (2004) Paleoenvironmental and paleoclimatic significance of freshwater bivalves in the Upper Jurassic Morrison Formation, Western Interior, USA. *Sed. Geol.*, **167**, 163–176.
- Gradstein, F.M., Ogg, J.G. and Smith, A.G.** (Eds) (2005) *A Geologic Time Scale 2004*. Cambridge University Press, Cambridge, 610 pp.
- Helmdach, F.F.** (1971) Stratigraphy and ostracod-fauna from the coalmine Guimarota (Upper Jurassic). *Mem. Serv. Geol. Portugal*, **17**, 41–88.
- Helmdach, F.F.** (1973) A contribution to the stratigraphical subdivision of nonmarine sediments of the Portuguese Upper Jurassic. *Comun. Serv. Geol. Portugal*, **57**, 5–26.
- Hill, G.** (1988) *The sedimentology and lithostratigraphy of the Upper Jurassic Lourinhã formation, Lusitanian Basin, Portugal*. Ph.D. dissertation, The Open University, Milton Keynes, UK, 292 pp.
- Hill, G.** (1989) Distal alluvial fan sediments from the Upper Jurassic of Portugal: controls on their cyclicity and channel formation. *J. Geol. Soc. Lond.*, **146**, 539–555.
- Jacquin, T., Dardeau, G., Durllet, C., de Graciansky, P.C. and Hantzpergue, P.** (1998) The North Sea cycle: an overview of 2nd-order transgressive/regressive facies cycles in western Europe. In: *Mesozoic and Cenozoic Sequence Stratigraphy of European Basins*, (Eds P.C. de Graciansky, J. Hardenbol, T. Jaquin and P.R. Vail), *SEPM Spec. Publ.*, **60**, 445–466.
- Keller, W.D.** (1970) Environmental aspects of clay minerals. *J. Sed. Petrol.*, **40**, 788–854.
- Kowallis, B.J., Christiansen, E.H. and Deino, A.L.** (1991) Age of the Brushy Basin Member of the Morrison Formation, Colorado Plateau, western USA. *Cretaceous Res.*, **12**, 483–493.
- Kowallis, B.J., Christiansen, E.H., Deino, A.L., Peterson, F., Turner, C.E., Kunk, M.J. and Obradovich, J.D.** (1998) The age of the Morrison Formation. *Mod. Geol.*, **22**, 235–260.
- Kriwet, J.** (2000) The fish fauna from the Guimarota mine. In: *Guimarota: A Jurassic Ecosystem* (Eds T. Martin and B. Krebs), pp. 41–50. Pfeil, Munich.
- Lapparent, A.F. and Zbyszewski, G.** (1957) Les dinosauriens du Portugal. *Mém. Serv. Géol. Portugal*, **2**, 1–63.
- Leinfelder, R.R.** (1986) Facies, stratigraphy and paleogeographic analysis of Upper? Kimmeridgian to Upper Portlandian sediments in the environs of Arruda dos Vinhos, Estremadura, Portugal. *Münchner Geowiss. Abh., A*, **7**, 1–215.
- Leinfelder, R.R.** (1993) A sequence stratigraphic approach to the Upper Jurassic mixed carbonate - siliciclastic succession of the central Lusitanian Basin, Portugal. *Profil*, **5**, 119–140.
- Leinfelder, R.R. and Wilson, R.C.L.** (1998) Third-order sequences in an Upper Jurassic rift-related second-order

- sequence, central Lusitanian Basin, Portugal. In: *Mesozoic and Cenozoic Sequence Stratigraphy of European Basins*, (Eds P.C. de Graciansky, J. Hardenbol, T. Jacquin and P.R. Vail), *SEPM Spec. Publ.*, **60**, 505–525.
- Mack, G.H.** and **James, W.C.** (1994) Paleoclimate and the global distribution of paleosols. *J. Geol.*, **102**, 360–366.
- Mack, G.H., James, W.C.** and **Monger, H.C.** (1993) Classification of paleosols. *Geol. Soc. Am. Bull.*, **105**, 129–136.
- Manuppella, G.** (1996) *Carta Geológica de Portugal 1/50,000. Folha 30-A, Lourinhã*. Instituto Geológico e Mineiro, Portugal.
- Manuppella, G.** (1998) Geologic data about the “Camadas de Alcobaça” (Upper Jurassic) north of Lourinhã, and facies variation. *Mem. Acad. Ciências Lisboa*, **37**, 17–24.
- Marques, B., Olóriz, F.** and **Rodrigues-Tovar, F.J.** (1996) Preliminary ecostratigraphic researches in the Middle-Upper Oxfordian from the Lusitanian Basin (West Portugal). Comparisons with the Eastern Algarve Basin (South Portugal). *C R Acad. Sci. Paris*, **322**, 757–764.
- Marriott, S.B.** and **Wright, V.P.** (1993) Palaeosols as indicators of geomorphic stability in two Old Red Sandstone alluvial suites, South Wales. *J. Geol. Soc. Lond.*, **150**, 1109–1120.
- Martinius, A.W.** and **Gowland, S.** (2011) Tide-influenced fluvial bedforms and tidal bore deposits (Late Jurassic Lourinhã Formation, Lusitanian Basin, Western Portugal). *Sedimentology*, **58**, 285–324.
- Mateus, O.** (2006) Late Jurassic dinosaurs from the Morrison Formation (USA), the Lourinhã and Alcobaça formations (Portugal), and the Tendaguru Beds (Tanzania): a comparison. *N.M. Mus. Nat. Hist. Sci. Bull.*, **36**, 223–231.
- Mateus, O., Walen, A.** and **Antunes, M.T.** (2006) The large theropod fauna of the Lourinhã Formation (Portugal) and its similarity to the Morrison Formation, with a description of a new species of *Allosaurus*. *N.M. Mus. Nat. Hist. Sci. Bull.*, **36**, 123–129.
- Maynard, J.B.** (1992) Chemistry of modern soils as a guide to interpreting Precambrian paleosols. *J. Geol.*, **100**, 279–289.
- Mohr, B.A.R.** (1989) New palynological information on the age and environment of Late Jurassic and Early Cretaceous vertebrate localities of the Iberian Peninsula (eastern Spain and Portugal). *Berl. Geowiss. Abh.*, **106**, 291–301.
- Mohr, B.A.R.** and **Schmidt, D.** (1988) The Oxfordian/Kimmeridgian boundary in the region of Porto de Mós (Central Portugal): stratigraphy, facies and palynology. *Neues Jb. Geol. Paläontol. Abh.*, **176**, 245–267.
- Nesbitt, H.W.** and **Young, G.M.** (1982) Early Proterozoic climates and plate motions inferred from major element chemistry of lutites. *Nature*, **299**, 715–717.
- Nordt, L., Orosz, M., Driese, S.G.** and **Tubbs, J.** (2006) Vertisol carbonate properties in relation to mean annual precipitation: implications for paleoprecipitation estimates. *J. Geol.*, **114**, 501–510.
- O’Sullivan, R.B.** (1992) The Jurassic Wanakah and Morrison formations in the Telluride-Ouray-Western Black Canyon area of southern Colorado. *Bull. US Geol. Surv.*, **1927**, 1–24.
- Parrish, J.T., Peterson, F.** and **Turner, C.E.** (2004) Jurassic “savannah”—plant taphonomy and climate of the Morrison Formation (Upper Jurassic, Western USA). *Sed. Geol.*, **167**, 137–162.
- Passey, B.H., Levin, N.E., Cerling, T.E., Brown, F.H.** and **Eiler, J.M.** (2010) High-temperature environments of human evolution in East Africa based on bond ordering in paleosol carbonates. *Proc. Natl Acad. Sci. USA*, **107**, 11245–11249.
- Pena dos Reis, R.P.B., Dinis, J.L., Proença Cunha, P.** and **Trincão, P.** (1996) Upper Jurassic sedimentary infill and tectonics of the Lusitanian Basin (western Portugal). *Geores. Forum* **1–2**, 377–386.
- Pena dos Reis, R.P.B., Proença Cunha, P., Dinis, J.L.** and **Trincão, P.R.** (2000) Geologic evolution of the Lusitanian Basin (Portugal) during the Late Jurassic. *Geores. Forum*, **6**, 345–356.
- Pereira, R., Feist, M.** and **Azerêdo, A.C.** (2003) New charophytes from the Upper Jurassic of the Lusitanian Basin (Portugal). *J. Micropalaeontol.*, **22**, 113–126.
- Peterson, F.** (1988) Stratigraphy and nomenclature of Middle and Upper Jurassic rocks, western Colorado Plateau, Utah and Arizona. *U.S. Geol. Surv. Bull.*, **1633-B**, 1–43.
- Peterson, F.** (1994) Sand dunes, sabkhas, streams, and shallow seas: Jurassic paleogeography in the southern part of the Western Interior Basin. In: *Mesozoic Systems of the Rocky Mountain Region, USA* (Eds M.V. Caputo, J.A. Peterson and K.J. Franczyk), pp. 233–272. The Rocky Mountain Section SEPM, Denver.
- Ravnås, R., Windelstad, J., Mellere, D., Nøttvedt, A., Stühr Sjøblom, T., Steel, R.J.** and **Wilson, R.C.L.** (1997) A marine Late Jurassic syn-rift succession in the Lusitanian Basin, western Portugal—tectonic significance of stratigraphic signature. *Sed. Geol.*, **114**, 237–266.
- Rees, P.M., Ziegler, A.M.** and **Valdes, P.J.** (2000) Jurassic phytogeography and climates: new data and model comparisons. In: *Warm Climates in Earth History* (Eds B.T. Huber, K.G. Macleod and S.L. Wing), pp. 297–318. Cambridge University Press, Cambridge.
- Retallack, G.J.** (1994) The environmental factor approach to the interpretation of paleosols. In: *Factors of Soil Formation: A Fiftieth Anniversary Retrospective, SSSA Special Publication, 33* (Ed H. Hari), pp. 31–63. Soil Science Society of America, Madison, WI.
- Royer, D.L.** (1999) Depth to pedogenic carbonate horizon as a paleoprecipitation indicator? *Geology*, **27**, 1123–1126.
- Savin, S.M.** and **Hsieh, J.C.C.** (1998) The hydrogen and oxygen isotope geochemistry of pedogenic clay minerals: principles and theoretical background. *Geoderma*, **82**, 227–253.
- Schudack, M.E.** (2000) Geological setting and dating of the Guimarota-beds. In: *Guimarota: A Jurassic Ecosystem* (eds T. Martin and B. Krebs), pp. 21–26. Pfeil, Munich.
- Schudack, M.E., Turner, C.E.** and **Peterson, F.** (1998) Biostratigraphy, paleoecology and biogeography of charophytes and ostracodes from the Upper Jurassic Morrison Formation, Western Interior, USA. *Mod. Geol.*, **22**, 379–414.
- Sellwood, B.W.** and **Valdes, P.J.** (2008) Jurassic climates. *Proc. Geol. Assoc.*, **119**, 5–17.
- Sheldon, N.D., Retallack, G.J.** and **Tanaka, S.** (2002) Geochemical climofunctions from North American soils and application to paleosols across the Eocene-Oligocene boundary in Oregon. *J. Geol.*, **110**, 687–696.
- Silverman, A.J.** and **Harris, W.L.** (1967) Stratigraphy and economic geology of the Great Falls-Lewistown coal field central Montana. *M.T. Bur. Mines Geol. Bull.*, **56**, 1–20.
- Singer, A.** (1984) The paleoclimatic interpretation of clay minerals in sediments—a review. *Earth-Sci. Rev.*, **21**, 251–293.
- Smith, A.G., Smith, D.G.** and **Funnell, B.M.** (1994) *Atlas of Mesozoic and Cenozoic Coastlines*. Cambridge University Press, Cambridge, 99 pp.
- Steiner, M.B.** (1998) Age, correlation, and tectonic implications of Morrison Formation paleomagnetic data, including rotation of the Colorado Plateau. *Mod. Geol.*, **22**, 261–281.

- Stern, L.A., Chamberlain, C.P., Reynolds, R.C. and Johnson, G.D.** (1997) Oxygen isotope evidence of climate change from pedogenic clay minerals in the Himalayan molasse. *Geochim. Cosmochim. Acta*, **61**, 731–744.
- Tabor, N.J. and Montañez, I.P.** (2005) Oxygen and hydrogen isotope compositions of Permian pedogenic phyllosilicates: Development of modern surface domain arrays and implications for paleotemperature reconstructions. *Palaeogeogr. Palaeoclimatol. Palaeoecol.*, **223**, 127–146.
- Tabor, N.J., Montañez, I.P. and Southard, R.J.** (2002) Paleoenvironmental reconstruction from chemical and isotopic compositions of Permo-Pennsylvanian pedogenic minerals. *Geochim. Cosmochim. Acta*, **66**, 3093–3107.
- Turner, C.E. and Fishman, N.S.** (1991) Jurassic Lake T'oo'dichi': a large alkaline, saline lake, Morrison Formation, eastern Colorado Plateau. *Geol. Soc. Am. Bull.*, **103**, 538–558.
- Turner, C.E. and Peterson, F.** (2004) Reconstruction of the Upper Jurassic Morrison Formation extinct ecosystem—a synthesis. *Sed. Geol.*, **167**, 309–355.
- Uchupi, E.** (1988) The Mesozoic-Cenozoic geologic evolution of Iberia, a tectonic link between Africa and Europe. *Rev. Soc. Geol. Esp.*, **1**, 257–294.
- Upchurch, P., Hunn, C.A. and Norman, D.B.** (2002) An analysis of dinosaurian biogeography: evidence for the existence of vicariance and dispersal patterns caused by geological events. *Proc. Roy. Soc. Lond. B*, **269**, 613–621.
- Valdes, P.J. and Sellwood, B.W.** (1992) A palaeoclimate model for the Kimmeridgian. *Palaeogeogr. Palaeoclimat. Palaeoecol.*, **95**, 47–72.
- Vitali, F., Longstaffe, F.J. and McCarthy, P.J.** (2002) Stable isotopic investigation of clay minerals and pedogenesis in an interfluvial paleosol from the Cenomanian Dunvegan Formation, N.E., British Columbia, Canada. *Chem. Geol.*, **192**, 269–287.
- Wilding, L.P. and Tessier, D.** (1988) Genesis of Vertisols: shrink-swell phenomena. In: *Vertisols: Their Distribution, Properties, Classification and Management. Developments in Soil Science*, 24 (Eds L.P. Wilding and R. Puentes), pp. 55–81. Texas A&M University Printing Center, College Station, TX.
- Wilson, R.C.L.** (1975) Atlantic opening and Mesozoic continental margin basins of Iberia. *Earth Planet. Sci. Lett.*, **25**, 33–43.
- Wilson, R.C.L.** (1979) A reconnaissance study of Upper Jurassic sediments of the Lusitanian Basin. *Ciências da Terra (UNL)*, **5**, 53–84.
- Wilson, R.C.L.** (1988) Mesozoic development of the Lusitanian Basin, Portugal. *Rev. Soc. Geol. Esp.*, **1**, 393–407.
- Wilson, R.C.L., Hiscott, R.N., Willis, M.G. and Gradstein, F.M.** (1989) The Lusitanian Basin of west-central Portugal: Mesozoic and Tertiary tectonic, stratigraphic, and subsidence history. In: *Extensional Tectonics and Stratigraphy of the North Atlantic Margins*, (Eds A.J. Tankard and H.R. Balkwill), *AAPG Memoir*, **46**, 341–361.
- Zhang, Y., Chen, W., Smith, S.L., Riseborough, D.W. and Cihlar, J.** (2005) Soil temperature in Canada during the twentieth century: Complex responses to atmospheric climate change. *J. Geophys. Res.*, **110**, D03112.

Manuscript received 13 May 2011; revision accepted 18 January 2012